Chemistry Europe
European Chemical Societies Publishing

WILEY VCH

Excellence in Chemistry Research

Announcing our new flagship journal

- Gold Open Access
- Publishing charges waived
- Preprints welcome
- Edited by active scientists

Meet the Editors of *ChemistryEurope*

Luisa De Cola
Università degli Studi di Milano Statale, Italy

Ive Hermans
University of Wisconsin-Madison, USA

Ken Tanaka
Tokyo Institute of Technology, Japan

Chemistry
A European
Journal

Chemistry Europe
European Chemical Societies Publishing

Accepted Article

Title: Isocyanides as Catalytic Electron Acceptors in the Visible Light Promoted Oxidative Formation of Benzyl and Acyl Radicals

Authors: Camilla Russo, Greta Donati, Francesco Giustiniano, Jussara Amato, Luciana Marinelli, Richard John Whitby, and Mariateresa Giustiniano

To be cited as: *Chem. Eur. J.* **2023**, e202301852

Link to VoR: https://doi.org/10.1002/chem.202301852

WILEY VCH

10.1002/chem.202301852

WILEY VCH

RESEARCH ARTICLE

Isocyanides as Catalytic Electron Acceptors in the Visible Light Promoted Oxidative Formation of Benzyl and Acyl Radicals

Camilla Russo,[a]† Greta Donati,[a]† Francesco Giustiniano,[b]† Jussara Amato,[a] Luciana Marinelli,[a] Richard John Whitby,[b] and Mariateresa Giustiniano*[a]

[a] Dr. C. Russo, Dr. G. Donati, Prof. J. Amato, Prof. L. Marinelli, and Prof. M. Giustiniano
Department of Pharmacy
University of Naples Federico II
via D. Montesano 49, 80131, Napoli
E-mail: mariateresa.giustiniano@unina.it

[b] Dr. F. Giustiniano and Prof. R. J. Whitby
School of Chemistry
University of Southampton
University Road, SO171BJ, Southampton, UK

Supporting information for this article is given via a link at the end of the document.

Abstract: The recent disclosure of the ability of aromatic isocyanides to harvest visible light and act as single electron acceptors when reacting with tertiary aromatic amines has triggered a renewed interest in their application to the development of green photoredox catalytic methodologies. Accordingly, the present work explores their ability to promote the generation of both alkyl and acyl radicals starting from radical precursors such as Hantzsch esters, potassium alkyltrifluoroborates, and α-oxoacids. Mechanistic studies involving UV-visible absorption and fluorescence experiments, electrochemical measurements of the ground-state redox potentials along with computational calculations of both the ground- and the excited-state redox potentials of a set of nine different aromatic isocyanides provided key insights to promote a rationale design of a new generation of isocyanide-based organic photoredox catalysts. Importantly, the green potential of the investigated chemistry has been herein demonstrated by a direct and easy access to deuterium labeled compounds.

Introduction

Isocyanides are the only class of stable organic compounds with a divalent carbon atom. This peculiarity accounts for their multiple reactivities, which could be considered as transitions from the carbon divalent state to the tetravalent state and vice versa.[1–4] While the two-electron chemistry of isocyanides has been massively investigated, in particular with the development of multicomponent reactions (MCRs) whose convergence accounts for their innate green nature,[5,6] less is known about their reactivity as geminal radical acceptors, probably due to the harsh reaction conditions required to generate open-shell species (i.e., high temperatures, stoichiometric initiators, and/or UV-light irradiation). Recent impressive progress of visible light photoredox catalysis has triggered a renewed consideration in the field[7–9] focussing on the mild generation of both carbon- and heteroatom- centered radicals by exploiting photons as a renewable energy source. Following our interest in the exploitation of isocyanide reactivity under visible light irradiation,[10] we recently came across the ability of aromatic isocyanides to harvest the energy of photons, reach an excited state, and ultimately act as single electron acceptors with aromatic tertiary amines (Figure 1a).[11,12] Based on this observation we carried out a range of metal-free *self-catalyzed* multicomponent reactions (*direct photochemistry*) with aliphatic isocyanides, without any additional photocatalyst, thanks to the formation of electron-donor/acceptor (EDA) complexes with the aromatic amines (Figure 1a). On the other hand, the potentiality of harnessing aromatic isocyanides as *catalytic organic photoactive oxidants* was further probed with a series of α-amino C(sp^3)-H functionalizations such as Michael addition, Strecker, Mannich, *aza*-Henry, and phosphonylation reactions (Figure 1a).[11] Prompted by promising preliminary results and fascinated by the opportunity of developing a new class of *visible light organic photocatalysts*, we report herein a theoretical and experimental study involving a selection of both alkyl- and acyl-radical precursors, characterized by different redox potentials and able to undergo oxidative photoredox cycles (Figure 1b). The species investigated involved Hantzsch esters, carboxylic acids, potassium alkyltrifluoroborates, and α-oxoacids. The oxidative fragmentation of such precursors often requires a metal-based photocatalyst, which upon excitation promotes a single electron transfer (SET) affording the corresponding open-shell species.[13] The thermodynamic feasibility of the isocyanide-promoted photoinduced electron transfer (PET)[14] was assessed by means of electrochemical measurements of the ground-state redox potentials along with computational calculations of both the ground and the excited-state redox potentials of a collection of aromatic isocyanides.

10.1002/chem.202301852

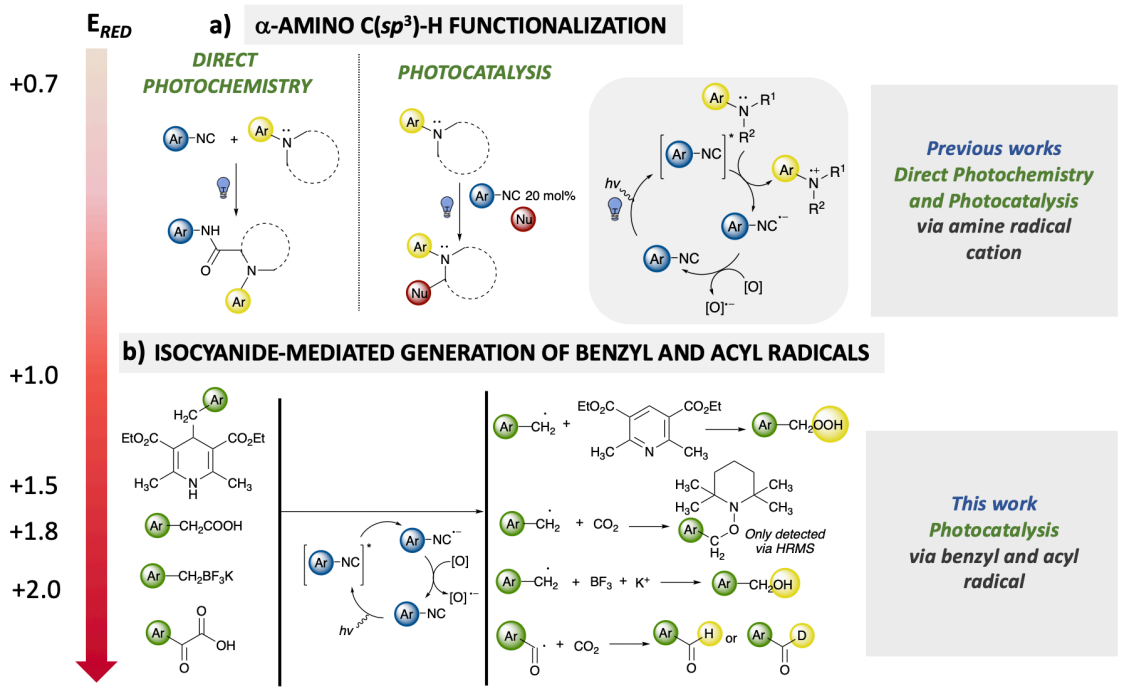

Figure 1. Isocyanides as photoactive catalytic single electron oxidant.

Carboxylic acids did not afford any product on a preparative scale, albeit the adduct of the corresponding alkyl radical with a radical quencher such as TEMPO [(2,2,6,6-tetramethylpiperidin-1-yl)oxyl] was detected by means of high-resolution mass spectrometry (HRMS). Further synthetic applications involved tandem one-pot multicomponent reactions, late-stage functionalization, and isotopic labelling. The results obtained, together with additional spectroscopic studies such as Stern-Volmer quenching analyses, provided key knowledge about the (re)activity of aromatic isocyanides as *organic catalytic single electron oxidants* under visible light irradiation conditions, which represent a green alternative to common oxidants such as halosuccinimides (*N*-chloro, *N*-bromo, and *N*-iodo-succinimide), Selectfluor®, persulfates, peroxides and peresters, halocarbons such as bromotrichloromethane, hypervalent iodine reagents, and transition metals.[13] Furthermore, the current study provided a fast and straightforward approach to valuable deuterium labeled compounds, via tandem one-pot multicomponent reactions and by using D_2O as a sustainable and readily available deuterium source

Results and Discussion

Based on the observation that isocyanide **1** (Figure 2) is able to promote the oxidation of tertiary aromatic amines (E_{red} +0.7-0.8 V *vs* SCE, on average) to amine radical cation, we wondered if such photoinduced electron transfer (PET) process could be extended to more challenging radical precursors (i.e., with higher redox potentials). The investigated species, listed in order of increasing redox potential, involve Hantzsch esters (E_{red} +1.0 V *vs* SCE, on average), carboxylic acids (carboxylate anion, E_{red} +1.5 V *vs* SCE, on average), potassium alkyltrifluoroborates (E_{red} +1.8 V *vs* SCE, on average), and α-ketoacids (carboxylate anion, E_{red} +2.0 V *vs* SCE, on average) (Figure 1b).

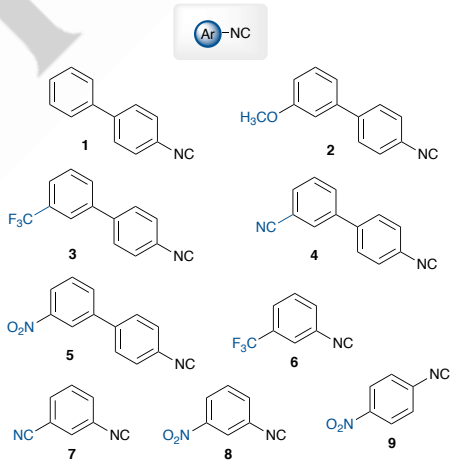

Figure 2. Library of isocyanides **1-9** synthesized for this work.

A library of eight analogues of isocyanide **1**, endowed with both electron- donor and withdrawing groups of various strengths, was designed and synthesized to obtain photocatalysts with different redox properties. Functional groups such as methoxy-, trifluoromethyl-, nitrile, and nitro-, on either biphenyl- (**2**-**5**, Figure 2) or aryl- moieties (**6**-**9**, Figure 2) were chosen. As the standard redox potential of an electron donor (i.e., radical precursors as in Figure 1) must match the redox properties of the electron acceptor, i.e., the aryl isocyanide, a preliminary evaluation of the redox properties of derivatives **1**-**9** was performed in order to explore the thermodynamic feasibility of a PET.

Theoretical and electrochemical studies. The ability of the aromatic isocyanides to promote a SET oxidation upon visible

10.1002/chem.202301852

light irradiation was at first investigated through a computational approach by computing the redox potentials of compounds **1-9** in both the ground (E°_{red}) and excited ($E^{\circ *}_{red}$) electronic state (Table 1) according to the procedure described in Supporting Information.

Table 1. Redox potentials of isocyanides **1-9** (V *vs* SCE), calculated ($E^{\circ}_{red}/E^{\circ *}_{red}$) and measured ($E_{1/2}$) via cyclic voltammetry (a: E_{pc}).

Ar–NC	E°_{red} Ground State (V vs SCE), calculated	$E^{\circ *}_{red}$ Excited State (V vs SCE), calculated	$E_{1/2}$ Ground State (V vs SCE), measured	$E_{1/2}$ Ground State residuals (V, measured – calculated)
1	-2.11	+ 1.63	-2.23	-0.12
2	-2.13	+ 1.79	-2.22	-0.09
3	-1.98	+ 1.80	-2.16[a]	-0.18
4	-1.69	+ 1.89	-2.02	-0.33
5	-0.86	+ 1.93	-1.10	-0.24
6	-2.11	+ 2.73	-2.29[a]	-0.18
7	-1.87	+ 2.56	-1.98[a]	-0.11
8	-0.71	+ 2.24	-0.96	-0.25
9	-0.66	+ 2.24	-0.95	-0.29

Density Functional Theory (DFT) was used for all the ground-state calculations and its time-dependent version (TD-DFT)[15-25] was employed for excited state properties, according to the procedure described in the Computational Methods Section. The calculated reduction potentials in acetonitrile are shown in Table 1 along with those measured by cyclic voltammetry (CV). The theoretical model was further corroborated by the CV measurements, which yielded redox potentials within 0.1-0.3 V of those obtained by calculation. The measurements were performed in CH_3CN/TBATFB/Ag-AgCl and in the absence of air and water, and referenced to the Ferrocene/Ferrocenium redox couple to obtain the standard redox potentials reported here *vs* SCE.

Reduction potentials in the ground state. The calculated reduction potentials in the ground state show a very good agreement with those measured by cyclic voltammetry (Table 1). This agreement is corroborated by the linear correlation found between the calculated and measured reduction potentials (Figure 3), showing an R^2 value of 0.989. More in detail, the isocyanide compounds appear to cluster in two different E°_{red} regions.

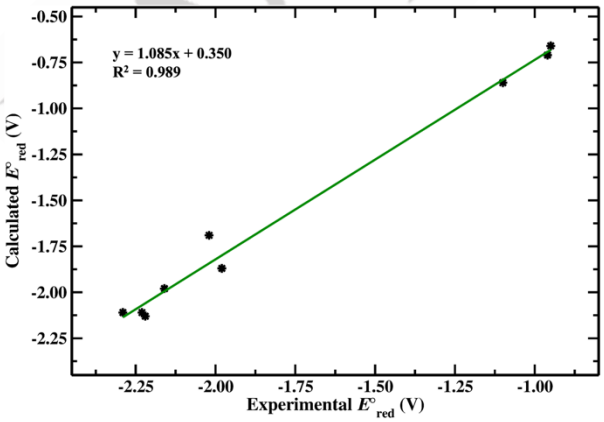

Figure 3. Linear correlation plot for the calculated and experimental ground-state redox potentials (V *vs* SCE) in acetonitrile.

Isocyanides **1**,**2**,**6** have poorer and similar oxidizing properties with calculated E°_{red} values in the range between -2.13 and -2.11 V, followed by compounds **3**,**4**,**7**. On the other side, compounds **5**,**8**,**9** show larger E°_{red}, spanning between computed values of -0.86 and -0.66 V *vs* SCE.

As firstly demonstrated by Maccoll[26] in 1949, the frontier molecular orbital energies and the redox potentials should be linearly correlated where, in particular, the reduction potentials are correlated with the energy of the Lowest Unoccupied Molecular Orbitals (LUMOs) while the oxidation potentials correlate with the Highest Occupied Molecular Orbitals (HOMOs). Thus, in Figure 4 the calculated E°_{red} are reported as function of the LUMO energies for all the isocyanide compounds. A well-defined linear correlation is detected, where the largest E°_{red} correspond to lowest LUMO energies and *vice versa*. This correlation is very powerful since allows to directly link the LUMO features to the redox potentials. In particular, in our case, a lower energy of the LUMOs is correlated to an easier capability of the isocyanide to accept an electron, resulting in better oxidizing properties of compounds **5**, **8**, and **9**. From Figure 4 it is clear that the decrease in LUMO energies depends on both the nature of the different functional groups and the nature of the aromatic scaffold (biphenyl or phenyl moieties). Electron-withdrawing substituent groups, especially the nitro group (**5** ,**8**, and **9**), have the largest capability of decreasing the LUMO energies, resulting in higher redox potentials.

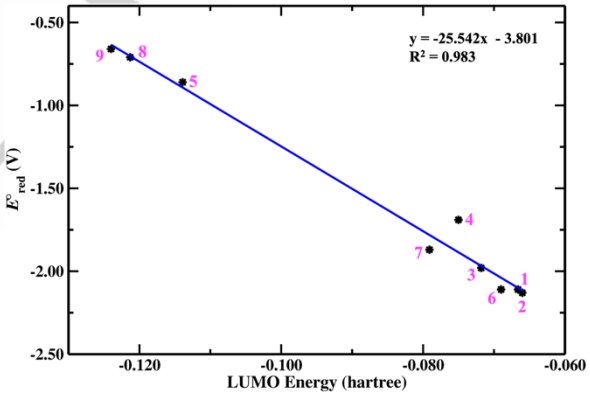

Figure 4. Correlation plot for the LUMO energies and the calculated ground-state redox potentials (V *vs* SCE) in acetonitrile.

By inspecting the LUMO isosurface plots (Figure 5), in compounds **5**, **8**, and **9** theelectronic density is withdrawn by the nitro group from the isocyanide moiety lowering their LUMO energies and thus favoring the gain of the incoming electron upon reduction. Conversely, the LUMO isosurfaces do not significantly change between the unsubstituted (**1**), methoxy (**2**) and the trifluoromethyl (**3**) substituted biphenyl compounds. The cyano-substituted compounds show a larger isodensity delocalization over such substituent groups, resulting in both lower LUMO energies and slightly better redox potentials for both the biphenyl (**4**) and phenyl (**7**) cases. These results suggest that the trifluoromethyl and cyano substituents are not able to lower the LUMO energy by efficiently delocalizing the electronic density and, in turn, cannot favor the reduction. From a structural point of view, the effect of the substituents is observed in terms of different

10.1002/chem.202301852

isocyanide bond lengths (see Table S6, Supporting Information), where the longest distance is found for compound **5**, confirming the capability of the nitro group to remove electronic density from the CN π bond. Regarding the N-C_{Ar} bond lengths, they do not change significantly among different compounds while the biphenyls are not co-planar in all compounds **1**-**5** (see Table S6, Supporting Information). The very good agreement found between the calculated and measured E°_{red} along with the capability to describe the linear correlation with LUMOs, further supports DFT as a reliable theory level to properly describe and predict the redox properties of these isocyanides.

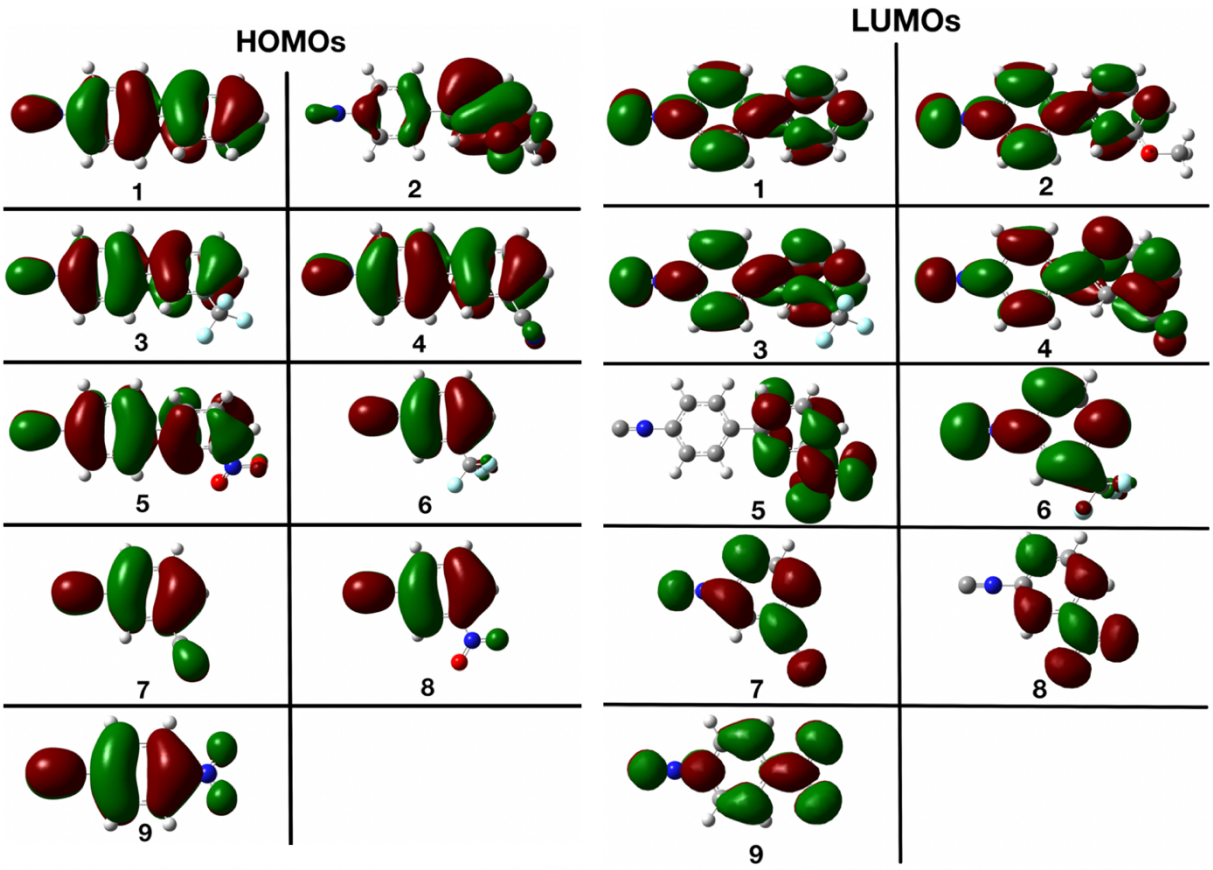

Figure 5. Isodensity surfaces evaluated for compounds **1**-**9** of the Highest Occupied Molecular Orbitals (HOMOs), left panels and Lowest Unoccupied Molecular Orbitals (LUMOs), right panels.

Reduction potentials in the excited state. The excited state reduction potentials ($E^{\circ *}_{red}$) were computed by TD-DFT calculations and applying the Latimer diagram (see Computational Methods in Supporting Information), and are reported in Table 1 for all the previously examined compounds. Upon excitation, the capability of isocyanides to act as oxidizing agents importantly increases in all the cases although to a different extent, demonstrating an overall capability of these isocyanides to act as photo-oxidants. Higher reduction potentials of the biphenyl compounds (**1**-**5**) in the excited state with respect to the ground state, could be related to the better capability to delocalize the charge, given the larger degree of co-planarity upon nuclear reorganization. In Table S6 (Supporting Information) are reported the inter-ring dihedral angles reaching values closer to planar configuration (±180º), and the inter-ring bond distances (CC), undergoing a shortening. Conversely, isocyanide bond distances (NC) increase and the bond between the isocyanide nitrogen atom and the carbon atom of the aromatic ring (NC_{Ar}) becomes shorter for all biphenyls (in a less extent for **5)**. These results suggest that the structural reorganization due to the electronic excitation, in terms of larger co-planarity and charge delocalization can improve the isocyanides' oxidizing abilities. We moved to the analysis of the electronic reorganization upon excitation by inspecting the isosurfaces of the involved molecular orbitals reported in Figure 5. Regarding compound **2,** a larger delocalization in the excited state can be witnessed by the LUMO density that is spread-out over the entire molecule with respect to the HOMO. However, as already discussed before, the methoxy substituent is not able to delocalize the charge, leading to a lower E°_{red} in comparison with the other compounds even in the excited state (see Table 1). Regarding compounds **3**, **4**, and **5** an increasing charge localization with respect to the ground state (see corresponding HOMO isoplots in Figure 5), is observed on the substituent groups. The nitro-substituted compound **5** presents the largest $E^{\circ *}_{red}$ among the biphenyl compounds in agreement with its largest electron-withdrawing capability. Regarding the phenyl compounds, an increase in the isocyanide bond length (NC) is observed (see Table S6, Supporting

10.1002/chem.202301852

RESEARCH ARTICLE

Information), suggesting a weakening of the bond most affecting compounds not carrying the nitro substituents, that remain almost unchanged (1.176 and 1.176 Å vs. 1.175 and 1.177 Å in the S_0 and S_1 states, respectively) for compounds **8** and **9**, respectively. The N-C_{Ar} bond distance undergoes a shortening for all isocyanides except than for **8** and **9**, where only the C-R bond distance is the most perturbed undergoing a decrease of ~0.1 Å. Overall, the phenyl compounds show the largest $E^{\circ}{}^{*}_{red}$. The HOMOs of **6**-**9** are delocalized on the aromatic ring and the isocyanide moiety while the LUMOs are delocalized also on the electron-withdrawing groups. In the phenyl rings, the effect of the substituents in influencing the electronic and nuclear properties in the excited state is emphasized with respect to the biphenyls, due to the absence of the conjugation that mitigates the effect of the substituent, leading to an improvement of their oxidizing properties. The nitro-, trifluoromethyl- and cyano-substituents give the biggest changes in the excited electronic state given their electron-withdrawing nature and larger capability in affecting the electronic reorganization upon excitation.

Synthetic studies involving Hantzsch esters. 4-Alkyl-1,4-dihydropyridines (DHPs, also known as Hantzsch esters) have been conveniently exploited as alkyl radical precursors thanks to a smooth oxidative fragmentation to form a fully aromatic pyridine (E_{red}= + 1.0 V *vs* SCE, on average). Furthermore, they are bench-stable solids, easily synthesized from widely available aliphatic aldehydes.[27–32] In order to evaluate the feasibility of a PET process mediated by an aromatic isocyanide, **10** was selected as a model substrate. Following the mechanistic hypothesis in Scheme 1, the latter, once oxidized via a SET mediated by the electronically excited isocyanide, should afford the benzyl radical **I**, which in the presence of a H-donor such as triisopropylsilane (TIS) could give 4-phenyltoluene **12**.

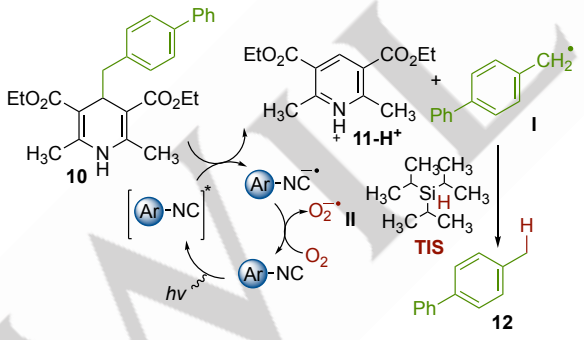

Scheme 1. Generation of radical **I** followed by H-abstraction to **12** (mechanistic design).

Nevertheless, when a test reaction was performed with a 20 mol% of isocyanide **8,** 1 equiv. of TIS, in acetonitrile (CH_3CN) as a solvent, and under irradiation with blue LEDs 30 W, at room temperature, overnight, the hydroperoxide **13** was formed in 47% yield (Entry 1, Table 2). The reaction was performed open to air in order to enabled the regeneration of the isocyanide ground state via oxidation of the isocyanide radical anion mediated by molecular oxygen. The use of TIS as an additive proved to be beneficial to the reaction, since its absence led to a poor outcome (Entry 2, Table 2), as well as the use of Hantzsch Ester (HE, diethyl 1,4-dihydro-2,6-dimethyl-3,5-pyridinedicarboxylate) as H-donor (Entry 3, Table 2), a different light source (Entries 4 and 5, Table 2), or the use of isocyanide **7** as the photocatalyst (Entry 6, Table 2).

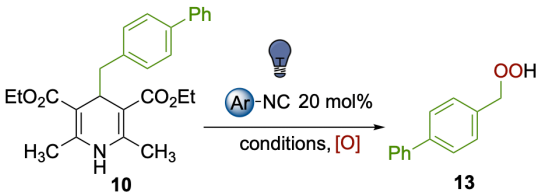

Entry	H-donor (1 equiv.)	Light source	Time (h)	Additive/ Catalyst	Yield[a] (%)
1	TIS	Blue LEDs 30 W	20	**8**	47
2	None	Blue LEDs 30 W	20	**8**	38
3	HE	Blue LEDs 30 W	20	**8**	16[b]
4	None	Blue LEDs 1 W	20	**8**	4.5
5	None	Blue LEDs 1 W	20	None	4
6	TIS	Blue LEDs 30 W	20	**7**	37
7	TIS	Blue LEDs 30 W	20	None	29[b]
8	TIS	Blue LEDs 30 W	48	**8**	58

Table 2. Reaction conditions for the formation of **13** (**10** (0.08 mmol), CH_3CN 0.15 M, RT, open-to-air, blue LEDs 450 nm; a: isolated yields; b: NMR yields).

Interestingly, the hydroperoxide **13** was obtained in a moderate yield (29%, Entry 7, Table 2) even in the absence of any catalyst, albeit **8** is able to promote its formation in 58% yield after 48 hours (Entry 8, Table 2). On the other hand, as for substrates other than benzylic ones, a test reaction performed with a Hantzsch Ester with a *n*-undecyl alkyl chain led to corresponding 1,4-DHP in 35%.

A working hypothesis for the formation of hydroperoxide **13** is depicted in Scheme 2, *path a*.

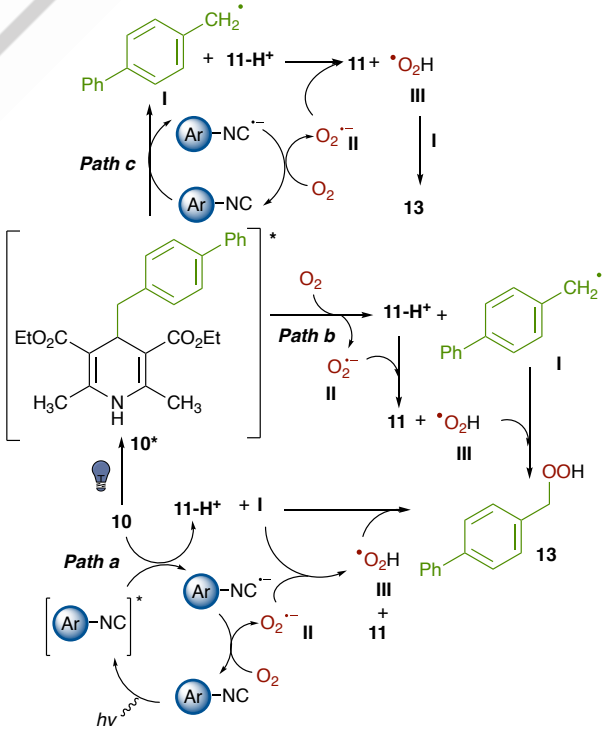

Scheme 2. Possible mechanist pathways for the formation of **13** (Self-coupling product not observed via NMR and HRMS analyses).

10.1002/chem.202301852

Its formation could hinge on a radical-radical coupling between **I** and the hydroperoxide radical **III** generated from molecular oxygen via 1) SET reduction to superoxide radical anion **II** followed by 2) proton abstraction from pyridinium ion **11-H$^+$**. Such hypothesis was further corroborated by the dramatic drop to 15 % and 7% yields when the reaction was performed in the presence of 1,4-benzoquinone (3 and 10 equivalents, respectively) as a superoxide radical anion scavenger.[33]

These results prompted us to investigate the UV-visible absorption properties of both **10** and **8** (Figure 6).

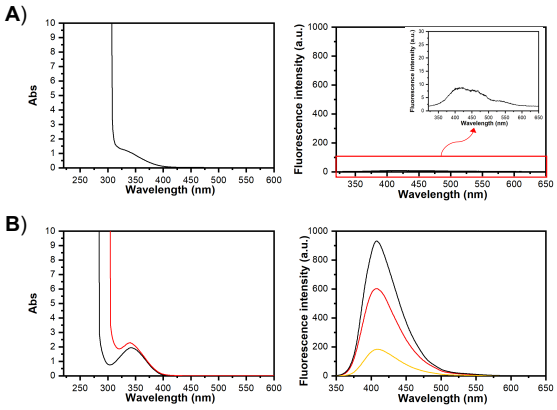

Figure 6. UV-visible absorption and fluorescence spectra for (A) **8**, and (B) **10** in the absence (black line) and presence of increasing amounts of **8** (10 and 50 equiv., red and yellow lines, respectively).

While it was not possible to measure a significant fluorescence band for isocyanide **8**, probably due to the nitro- functional group acting as an intramolecular fluorescence quencher,[34,35] the absorption bands in the visible light region for both **8** and **10**, along with a fluorescence peak (λ_{exc}=343) for **10** provided experimental data to support *path b* (in the absence of **8**, Scheme 2) and either *path a* or *path c* (Scheme 2), both promoted by a catalytic amount of **8**.

In *path b* **10** is able to absorb a photon and reach an electronically excited state, which was quenched by molecular oxygen to give a superoxide radical anion **II**, the benzyl radical **I**, and the pyridinium cation **11-H$^+$**. Deprotonation of the latter by the superoxide radical anion **II** provided a hydroperoxide radical **III**, which was able to quench the benzyl radical **I** in a radical-radical coupling to give **13**. On the other hand, when isocyanide **8** is present in the reaction mixture, it could either act as a *photoactive catalyst*, and upon excitation promote a SET oxidation of **10** (*path a*, Scheme 2), or behave as a *sacrificial catalytic electron-acceptor* (*path c*, Scheme 2). This mechanistic path was supported by the Stern-Volmer quenching experiments (Figure 6) where **8** is able to completely quench the fluorescence peak of **10**.

Synthetic studies involving potassium alkyltrifluoroborates. The exploitation of potassium alkyltrifluoroborates as alkyl radical precursors has been pioneered in 2014 by Prof. G. Molander in a photoredox/nickel dual catalytic formation of C(sp^2)-C(sp^3) bonds. This first seminal report set the stage for a wide range of processes involving catalytic single-electron oxidative fragmentation of alkyltrifluoroborates.[36–38] Besides iridium and ruthenium polypyridyl complexes, it has been shown that photoorganocatalysts such as MesAcr ($E_{1/2}$ P*/P$^-$ = + 2.06 V *vs* SCE), 4CzIPN ($E_{1/2}$ P*/P$^-$ = + 1.35 V *vs* SCE), and Eosin Y ($E_{1/2}$ P*/P$^-$ = + 0.83 V *vs* SCE) could be harnessed to promote the generation of alkyl radical species from alkyltrifluoroborates. Prompted by the preliminary results achieved with the Hantzsch ester **10**, and considering the desirable features of alkyltrifluoroborates such as commercially availability, convenient synthesis on a multi-gram scale, good functional group tolerance, and reasonable oxidation potential, we engaged in the investigation of a PET promoted by aryl isocyanides. To this end, potassium ([1,1'-biphenyl]-4-ylmethyl)trifluoroborate **14** was synthesized and irradiated with 30 W blue LEDs in a CH_3CN/H_2O 8:2 solvent mixture, in the presence of isocyanide **8** (20 mol%) and TIS as a H-donor, at room temperature for 20 hours. Again, the expected product, 4-phenyltoluene **12**, was not observed while alcohol derivative **15** was isolated in 65% yield (Entry 1, Table 3). The use of TIS as an additive proved to be beneficial (Entry 2, Table 3), albeit a further increase to 2 equivalents led to poorer results (Entry 3, Table 3). The screening of different solvents (Entries 4-7, Table 3), as well as HE as a H-donor (Entry 8, Table 3), isocyanide **7** as a photoactive single-electron oxidant (Entry 9, Table 3), and longer reaction times (Entry 10, Table 3) did not produce better outcomes. Differently from HE **10**, in this case the presence of an aryl isocyanide such as **8** was mandatory to promote the formation of **15** (Entry 11, Table 3). Alkyl trifluoroborates other than benzylic ones failed to afford the corresponding alcohols with most of the starting material recovered.

Table 3. Reaction conditions for the formation of **15** (**14** (0.08 mmol), solvent 0.15 M, light source: blue LEDs 30 W, open-to-air; a: 1 equiv.; b: isolated yields; c: 2 equiv.; d: NMR yields; e: 48 h).

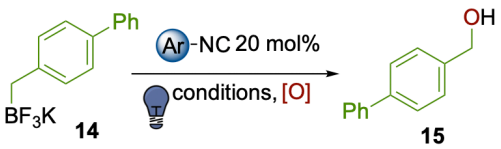

Entry	H-donor[a]	Solvent	Catalyst	Yield (%)[b]
1	TIS	MeCN/H_2O 8:2	**8**	65
2	None	MeCN/H_2O 8:2	**8**	50
3	TIS[c]	MeCN/H_2O 8:2 (0.15 M)	**8**	52
4	TIS	MeCN/H_2O 3:1	**8**	25[d]
5	TIS	MeCN/H_2O 9:1	**8**	45[d]
6	TIS	MeOH	**8**	60
7	TIS	*i*PrOH	**8**	49
8	HE	MeCN/H_2O 8:2	**8**	58
9	TIS	MeCN/H_2O 8:2	**7**	32
10[e]	TIS	MeCN/H_2O 8:2	**8**	42
11	TIS	MeCN/H_2O 8:2	None	ND

10.1002/chem.202301852

Based on these results, a mechanistic hypothesis for the formation of **15**, supported by fuorescence quenching analysis, is depicted in Scheme 4: the electronically excited isocyanide **8** is able to promote a SET oxidation of potassium alkyltrifluoroborate **14**, further undergoing a fragmentation to benzyl radical **I**, boron trifluoride (BF_3), and a potassium ion (K^+). The regeneration of the ground state **8** by molecular oxygen led to the formation of a superoxide radical anion $O_2^{\bullet-}$ **(II)**, which abstracted a hydrogen atom from either TIS or H_2O to give hydroperoxide anion HO_2^- **(III)**, then protonated by excess water to hydrogen peroxide H_2O_2 **(IV)**. Further SET reduction of the latter could lead to hydroxyl radical $OH^{\bullet}$ **(V)**, which could undergo a radical-radical coupling with **I** to give the alcohol **15**. **15** could also form upon addition of radical **I** to molecular oxygen albeit we did not observe it when starting from HE **10**. In theory, the electron donor could be either the reduced catalyst $\mathbf{8}^{\bullet-}$, thus regenerating **8**, or **14** in a chain formation of **I**. However, any attempts of forming **15** by reacting **14** in hydrogen peroxide (either 3% or 30%, both in absence and in the presence of light) led to exclude the latter hypothesis while the comparison between the redox potential of hydrogen peroxide ($E°$ H_2O_2/ $OH^{\bullet}$ = + 0.39 V *vs* NHE, + 0.24 V *vs* SCE) and the redox couple $\mathbf{8}/\mathbf{8}^{\bullet-}$ ($E_{1/2}$= - 0.71 V *vs* SCE) further supported the role of $\mathbf{8}^{\bullet-}$ as single electron donor.

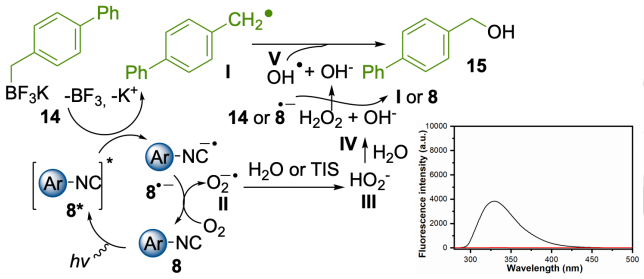

Scheme 4. Mechanistic hypothesis for the formation of **15**. Fluorescence spectra of **14** in the absence (black line) and presence (red line) of **8** (10 equiv.) (Self-coupling product not observed via NMR and HRMS analyses).

Synthetic studies involving α-ketoacids. The first report about the involvement of α-ketoacids as acyl radical precursors in a decarboxylative homolytic acylation dates back to 1972, when prof. Minisci reported a silver catalyzed synthesis of pyridine and pyrazine derivatives.[39] In the last decade, the impressive progresses in the field of visible-light photoredox catalysis have been involved the application of α-ketoacids to the decarboxylative/ oxidative synthesis of amides,[40] the hydroacylation of dialkyl azodicarboxylates,[41] the direct synthesis of ketones,[42] and decarboxylative ynonylation reactions,[43] to cite a few.[44] While most of these synthetic protocols require the use of metal-based photocatalysts, we wondered whether an aromatic isocyanide such as **6**-**8** could be harnessed to promote the oxidative decarboxylation of phenylglyoxylic acid **16** to the acyl radical **17**, which could then undergo a hydrogen atom abstraction to give an aldehyde derivative **18** (Scheme 5a).

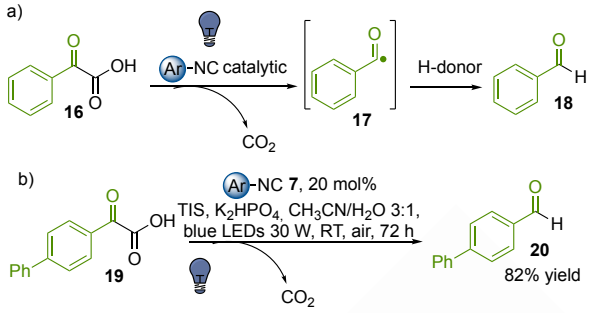

Scheme 5. Visible light promoted formation of aldehydes from α-ketoacids.

To this end, different additives such as TIS and HE, solvents (i.e., CH_3CN/H_2O mixtures), and reaction times were investigated (see Table 4 and Table S1 in Supporting Information) by monitoring the residual **16** via NMR spectroscopy. A 60% conversion was observed in the presence of isocyanide **7** (20 mol%), TIS (1 equiv.), K_2HPO_4 (1.2 equiv.), in a CH_3CN/H_2O 3:1 solvent mixture (0.25 M), at room temperature, under irradiation with 30 W blue LEDs for 72 hours. The application of the optimum reaction conditions to 2-([1,1'-biphenyl]-4-yl)-2-oxoacetic acid **19** enabled the isolation of the aldehyde **20** in 82% yield (Scheme 5b). Interestingly, similar results were obtained in the absence of **7** (71% yield), while TIS, as well as the light source, proved to be essential to promote the reaction (Table 4).

Table 4. Optimization of the reaction conditions for the synthesis of aldehyde **20** (Reaction performed on 0.08 mmol scale of **19**; Solvent: MeCN/H_2O 3:1 (0.25 M), K_2HPO_4 (1.2 equiv.), light source: blue LEDs 30 W, RT, 72 h; a: determined by NMR; b: in the dark).

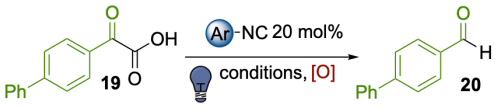

Entry	Additive (1 equiv.)	Catalyst	Yield[a]
1	TIS	7	82%
2	TIS	No one	71%
3	No one	7	58%
4	TIS	7	10%[b]
5	TIS	No one	8%[b]

The generality of such transformation as well as the beneficial effects of isocyanide **7** were further probed by conversion of the corresponding α-ketoacids to aldehydes **21**-**24**, in the presence of both electron-donor and electron-withdrawing groups (Scheme 6a). Furthermore, the mild reaction conditions enabled the interception in situ of the aldehydes in a range of tandem one-pot multicomponent transformations, such as the Passerini 3-CR, the Strecker 3-CR, and the Ugi-tetrazole 4-CR. Interestingly, the presence of isocyanide **7** exerted a more pronounced influence on the yields of the multicomponent products as shown for the Passerini 3-CR adduct **25** (58% yield in the presence of 20 mol% **7**; 26% yield in the absence of **7**). Examples **27** and **28** involved the late-stage functionalization[45] of cholic acid and gemfibrozil to form the ester derivatives in 32% and 23% yields, respectively (Scheme 6b).

10.1002/chem.202301852

RESEARCH ARTICLE

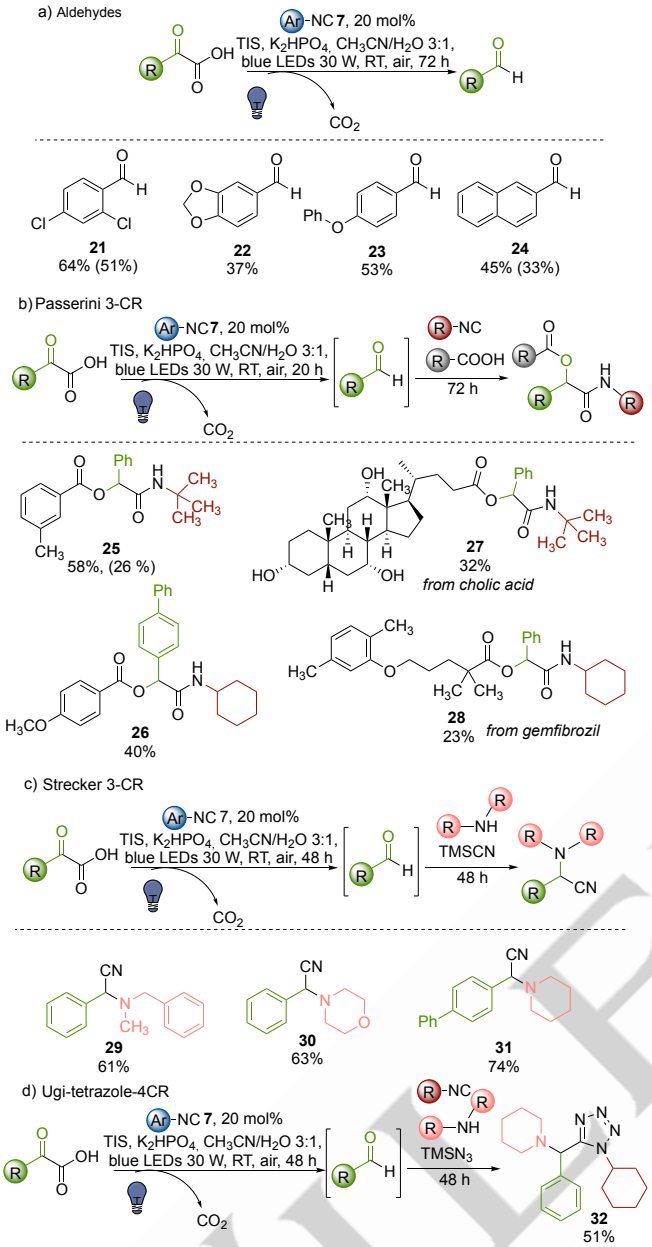

Scheme 6. Visible light promoted synthesis of aldehydes **21-24** and tandem MCRs (yields in parentheses were obtained in the absence of **7**).

The moderate yields obtained could be due to a slow reaction in the solvent system (CH_3CN/H_2O) required for the photocatalytic step as the comparison with a P-3CR starting from benzaldehyde and performed in the same solvent mixture led to the same identical yield of 58% for products **25** (See also Experimental Section). The P-3CR is indeed known to be favored in apolar aprotic solvents such as dichloromethane. A small library of α-aminonitriles **29-31** was obtained by adding to the aldehyde formed in situ either a linear or a cyclic secondary aliphatic amine and cyanotrimethylsilane (TMSCN, Scheme 6c), while the tetrazole **32** was formed upon addition of piperidine, cyclohexyl isocyanide, and azidotrimethyl silane in an Ugi-tetrazole 4-CR (Scheme 6d). Worthy of note, the yields obtained from the tandem decarbonylative aldehyde formation/MCR were comparable to those obtained starting directly from the aldehydes (e.g., S3-CR for product **29**: 85% NMR yield starting from benzaldehyde and 73% NMR yield with the tandem one-pot method starting from α-ketoacids; UT4-CR for product **32**: 63% NMR yield starting from benzaldehyde and 80% NMR yield with the tandem one-pot method starting from α-ketoacids; see Experimental Section).

While decarboxylative acyl radical formation as well as decarbonylative alkyl radical generation have been reported, to our knowledge this is the first synthetic methodology where the ketoacid carbonyl C(sp^2) ends up in a C(sp^3) without requiring net-reducing conditions. In order to provide experimental data supporting a working mechanistic hypothesis for the formation of aldehydes **21-24**, UV-visible absorption as well as fluorescence measurements were performed (Figure 7).

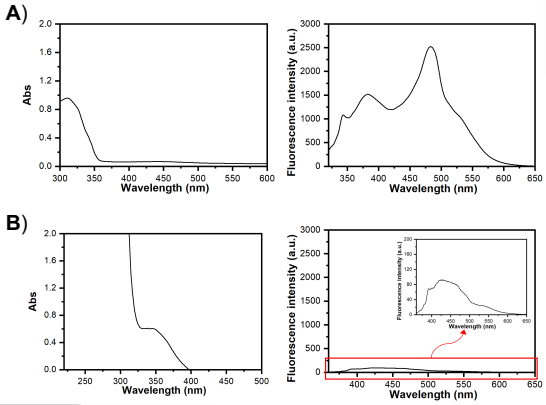

Figure 7. UV-vis absorption and fluorescence spectra of (A) isocyanide **7** and (B) phenylglyoxylic acid **16**.

On the basis of such experiments, it was reasonable to propose the formation of the aldehyde derivatives in the absence of **7** as due to the ability of phenylglyoxylic acid **16** to absorb a photon and reach an electronically excited state (Scheme 7, path a). The latter could be quenched by molecular oxygen to form the open-shell species **17** and the superoxide radical anion $O_2^{\bullet-}$ **(II)**, followed by hydrogen atom abstraction to give the aldehyde **18**.

When the reaction was performed in the presence of the isocyanide, two reaction mechanisms could possibly lead to the observed increase in the yield of **18**, where **7** could act either as a *photoactive single electron oxidant* (Scheme 7, path b) or a *sacrificial catalytic single electron acceptor* (Scheme 7, path c).

10.1002/chem.202301852

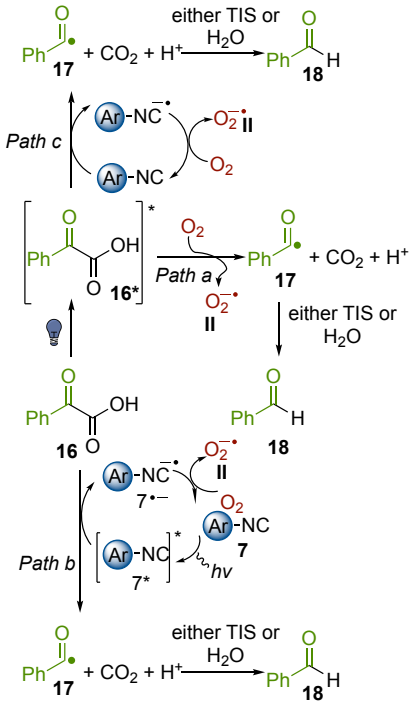

Scheme 7. Mechanistic hypotheses for the formation of aldehyde **18**.

Path b was further supported by Stern-Volmer fluorescence quenching of **7** observed by addition of increasing amounts of **16** (Figure 8).

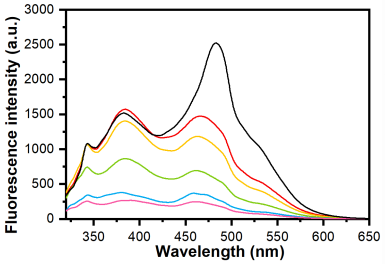

Figure 8. Stern-Volmer quenching of **7** (black line) via addition of increasing amounts of **16** (0.1, 0.2, 0.4, 0.8 and 1.0 equiv., red, yellow, green, cyano, and magenta lines, respectively).

The hydrogen atom source was identified via formation of the labelled **20-D** (87% yield, 98% deuteration) when water was replaced by deuterium oxide (D_2O, Scheme 8a).[46] The high percentage of deuterium labeling led to exclude the role of TIS as a hydrogen atom donor.

On the other hand, a test reaction performed in the absence of TIS afforded a decreased yield (78%) while not changing the isotopic labeling (98%, Scheme 8b), thus excluding its role as a deuterium atom transfer catalyst. This observation was further corroborated by the comparison between the 1H-NMR spectra of TIS in acetonitrile alone and after the addition of deuterium oxide and irradiation with blue LEDs for 20 h, which revealed that any Si-*H*/Si-*D* exchange took place (see Supporting Information). When the reaction was performed in the presence of deuterated acetonitrile (CH_3CN-d_3, Scheme 8c), **20** was obtained in 72% yield while no deuterated product **20-D** was observed. The possibility to get deuterium labeled aldehydes was further tested by converting the corresponding α-ketoacids into **21-D** and **24-D**.

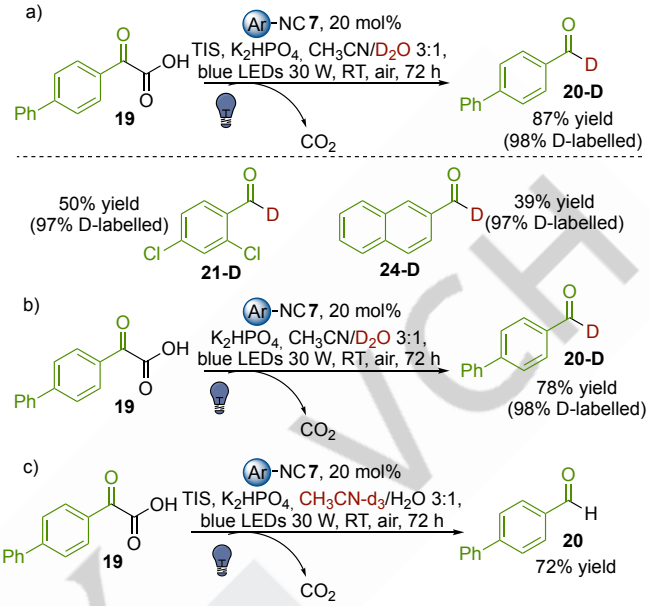

Scheme 8. Deuterium labelling experiments.

Deuterium incorporation into bioactive compounds has been proved as a valuable tool to slow down drug metabolism, optimize the pharmacokinetic properties, reduce the toxicity by either reducing the formation of unwanted metabolites or increasing the formation of active ones (metabolic shunting), and stabilize chemically unstable stereoisomers as shown for thalidomide.[47] Furthermore, deuterated drugs could be key in the elucidation of the mechanism of action and in the development of PET tracers. Since the FDA approval of deutetrabenazine in 2017 to treat choreas associated with Huntington's disease, a good number of derivatives have reached clinical trials. Notwithstanding their therapeutic value, deuterium-labeled drugs are currently obtained via poor synthetic approaches such as 1) conventional multistep routes starting from expensive deuterated reagents and 2) isotope exchange, including reductive deuteration in the presence of D_2 gas. Prompted by the urgent need of identifying a straightforward, green, and direct access to deuterated drug-like compounds, we wondered if the developed SET oxidation/H-abstraction sequence affording D-labelled aldehydes could be exploited in tandem one-pot multicomponent reactions. To this end, the Passerini 3-CR (Scheme 9a), the Strecker 3-CR (Scheme 9b), and the Ugi-tetrazole 4-CR (Scheme 9b) were selected as model MCRs: after visible light triggered formation of aldehydes **20-D** and **18-D**, the corresponding reactants (*t*-butyl isocyanide and *m*-toluic acid for the P3-CR, *N*-benzylmethylamine and TMSCN for the S3-CR, and cyclohexyl isocyanide, piperidine, and $TMSN_3$ for the UT4-CR) were added in situ and reacted at room temperature for 48-72 hours, leading to the formation of C(sp^3)-D bonds as in products **33-D**, **29-D**, and **32-D**, respectively, in good yields and excellent deuterium labelling.

10.1002/chem.202301852

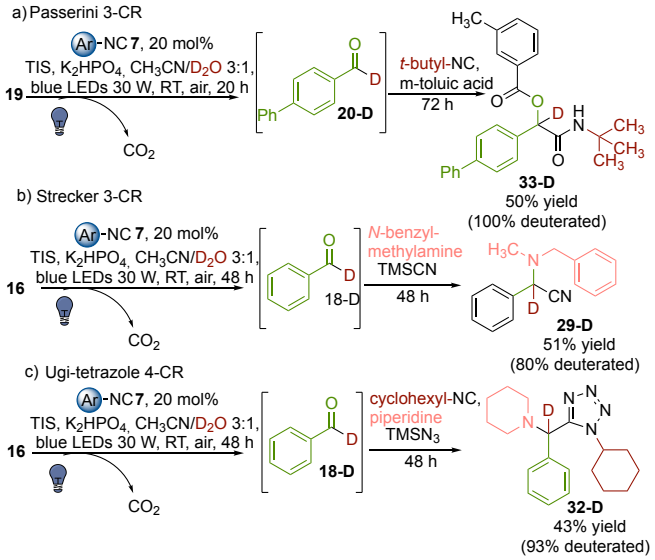

Scheme 9. Tandem one-pot visible light photocatalytic SET oxidation/H-abstraction/MCRs to D-labelled derivatives **33-D**, **29-D**, and **32-D**.

To our knowledge, this is the first report of a one-pot multicomponent conversion of a C(sp^2)-C(sp^2) bond into a C(sp^3)-D bond. The visible light photocatalytic method herein developed is endowed with ease-of-use and versatility, and it can afford diverse and complex analogues in short times and with higher yields compared to multistep routes, thus enabling a direct access to deuterated compounds starting from readily available α-ketoacids and using green and inexpensive deuterium oxide as the deuterium source.

Conclusion

In conclusion, thanks to their synthetic accessibility and the ease of functionalization, aromatic isocyanides could represent a novel class of visible light photoactive single electron acceptors. In this context, we investigated here the ability of representative aromatic isocyanides to promote the oxidation of substrates with increasing redox potentials, such as Hantzsch esters, potassium alkyltrifluoroborates, and α-oxoacids. Experimental results showed that this class of compounds could be considered as an organic catalytic green alternative to either metal-based photoredox catalysts or to stoichiometric oxidants such as halosuccinimides, persulfates, peroxides, and hypervalent iodine reagents, in case of photoactive radical precursors. Theoretical studies involving the calculation of both the ground- and the excited-state redox potentials, as well as the analysis of the HOMO and LUMO energies, indicated a marked increase in the isocyanides oxidizing ability upon excitation. The level of theory used was further validated by electrochemical measurements of the isocyanides ground state redox potential. Further investigations based on UV-visible absorption and fluorescence quenching experiments supported the mechanistic hypotheses. Worthy of note, the mild reaction conditions enabled a direct and smooth deuterium incorporation into both aldehydes and more complex multicomponent products, leading to C(sp^2)-D and C(sp^3)-D bonds formation starting from cheap and readily available deuterium oxide as deuterium source.

Experimental

General methods for synthesis. Commercially available reagents and solvents were used without further purification. Photochemical reactions were carried out using a PhotoRedOx Box (EvoluChem™) with 30 W blue LEDs (EvoluChem™, model: HCK1012-01-008, wavelength 450 nm, LED: CREE XPE. A holder suitable for 4 ml scintillation vials (45 x 14.7 mm) has been fitted within the box: this allowed a fixed sample placement distance from the light source). All NMR spectra were obtained with Bruker Avance NEO 400, 600 or 700 MHz instruments. Experiments for structure elucidation were performed in $CDCl_3$ at 25 °C with a RT-DR-BF/1H-5mm-OZ SmartProbe. High-resolution ESI-MS spectra were performed on a Thermo LTQ Orbitrap XL mass spectrometer. The spectra were recorded by infusion into the ESI source using MeOH as the solvent. Chemical shifts (δ) are reported in part per million (ppm) relative to the residual solvent peak. Column chromatography was performed on silica gel (70–230 mesh ASTM) using the reported eluents. Thin layer chromatography (TLC) was carried out on 5 x 20 cm plates with a layer thickness of 0.25 mm (Silica gel 60 F_{254}) to monitor the reaction by using UV as the revelation method.

Synthesis and Characterization Data of the Isocyanides. General Procedure A for the Synthesis of Compounds 1, 7-9.[48] In a 50 mL two-necked round bottom flask, a mixture of formic acid (2.7 equiv.) and acetic anhydride (2.3 equiv.) was stirred at 55°C for 2 h. After the reaction was cooled at room temperature, the crude mixture was added dropwise to a solution of the starting amine (1 equiv.) in THF (0.6 M) at 0° C. The resulting mixture was stirred at room temperature for 2 h, until the completion of the reaction, as monitored by TLC. Then the reaction was cooled to 0° C and a saturated aqueous solution of $NaHCO_3$ was added slowly under vigorous stirring, until neutral pH was reached. EtOAc was added, and the two phases were separated; the aqueous layer was further extracted with EtOAc (x2), then the combined organic extracts were washed with brine, dried over sodium sulfate, filtered, and concentrated under reduced pressure to give the resulting formamide in quantitative yield. The crude material was used in the next step without further purification. In a 100 ml round bottom flask equipped whit a magnetic stir bar, the formamide was dissolved in THF (0.6 M), and TEA (6.7 equiv.) was added to the solution. After cooling to 0°C, phosphorus oxychloride (1.7 equiv.) was added dropwise under argon atmosphere to the reaction mixture, which was stirred at room temperature for 1 h. After the completion of the reaction, as monitored by TLC, the mixture was cooled to 0° C and a saturated aqueous solution of Na_2CO_3 was added slowly under vigorous stirring, until pH ~ 9. Then CH_2Cl_2 was added, and the two phases were separated; the aqueous layer was further extracted with CH_2Cl_2 (x2), then the combined organic extracts were washed with brine, dried over sodium sulfate, filtered, concentrated under vacuum, and the crude mixture was purified by silica gel chromatography.

General Procedure B for the Synthesis of Compounds 2-4. *N*-biaryl formamides were prepared following a literature procedure

10.1002/chem.202301852

reported by Lipshutz et al.,[49] and then dehydrated according to standard methods[1] to afford the desired isocyanides **2-4**. Pd(dtbpf)Cl_2 (2 mol %), arylboronic acid (1.5 equiv.) and *N*-(4-bromophenyl)formamide (1 equiv.) were added under argon to a 50 mL round bottom flask equipped with a magnetic stir bar. Aqueous TPGS-750-M (2% w/w, 0.5 M) and Et_3N (3 equiv.) were then added via syringe while vigorously stirring. The reaction mixture was stirred overnight at 50° C. Upon completion of the reaction, as monitored by TLC, the crude mixture was diluted with brine and extracted with EtOAc (x3). The organic extracts were dried over sodium sulfate, filtered, concentrated under vacuum, and the crude product was purified by silica gel column chromatography. The resulting *N*-biaryl formamide was then dissolved in THF (0.6 M), and TEA (6.7 equiv.) was added to the solution. After cooling to 0°C, phosphorus oxychloride (1.7 equiv.) was added dropwise under argon atmosphere to the reaction mixture, which was stirred at room temperature for 1 h. After the completion of the reaction, as monitored by TLC, the mixture was cooled to 0° C and a saturated aqueous solution of Na_2CO_3 was added slowly under vigorous stirring, until pH ~ 9. Then CH_2Cl_2 was added, and the two phases were separated; the aqueous layer was further extracted with CH_2Cl_2 (x2), then the combined organic extracts were washed with brine, dried over sodium sulfate, filtered, and concentrated under vacuum. The crude mixture was purified by silica gel chromatography.

Procedure C for the Synthesis of Compound 5. *N*-(3'-nitro-[1,1'-biphenyl]-4-yl)formamide was prepared following the literature procedure reported by Lipshutz et al.,[49] and then dehydrated according to the method developed by Dömling et al.[50] to afford the desired 4'-isocyano-3-nitro-1,1'-biphenyl ***5***. Pd(dtbpf)Cl_2 (2 mol %), (3-nitrophenyl)boronic acid (1.5 equiv.) and *N*-(4-bromophenyl)formamide (1 equiv.) were added under argon to a 50 mL round bottom flask equipped with a magnetic stir bar. Aqueous TPGS-750-M (2% w/w, 0.5 M) and Et_3N (3 equiv.) were then added via syringe while vigorously stirring. The reaction mixture was stirred overnight at 50° C. Upon completion of the reaction, as monitored by TLC, the crude mixture was diluted with brine and extracted with EtOAc (x3). The organic extracts were dried over sodium sulfate, filtered, and concentrated under vacuum, and the crude product was purified by silica gel column chromatography. The resulting *N*-(3'-nitro-[1,1'-biphenyl]-4-yl)formamide was then suspended in CH_2Cl_2 (0.2 M), and TEA (5 equiv.) was added to the suspension. After cooling to 0°C, phosphorus oxychloride (1 equiv.) was added dropwise under argon atmosphere to the reaction mixture, which was stirred at room temperature for 1 h. After the completion of the reaction, as monitored by TLC, the crude mixture was transferred into a column pre-packed with dry 100-200 mesh size silica, and the isocyanide was eluted with Et_2O.

Procedure D for the Synthesis of Compound 6. *N*-(3-(trifluoromethyl)phenyl)formamide was prepared according to the standard procedure[1] and then dehydrated following the method developed by Dömling et al.[50] to afford the desired 1-isocyano-3-(trifluoromethyl)benzene **6**. In a 50 mL two-necked round bottom flask, a mixture of formic acid (2.7 equiv.) and acetic anhydride (2.3 equiv.) was stirred at 55°C for 2 h. After the reaction was cooled at room temperature, the crude mixture was added dropwise to a solution of the starting amine (1 equiv.) in THF (0.6 M) at 0° C. The resulting mixture was stirred at room temperature for 2 h, until the completion of the reaction, as monitored by TLC. Then the reaction was cooled to 0° C and a saturated aqueous solution of $NaHCO_3$ was added slowly under vigorous stirring, until neutral pH was reached. EtOAc was added, and the two phases were separated; the aqueous layer was further extracted with EtOAc (x2), then the combined organic extracts were washed with brine, dried over sodium sulfate, filtered, and concentrated under reduced pressure to give the resulting formamide in quantitative yield. The crude material was used in the next step without further purification. In a 100 ml round bottom flask equipped whit a magnetic stir bar, the formamide was suspended in CH_2Cl_2 (0.2 M), and TEA (5 equiv.) was added to the suspension. After cooling to 0°C, phosphorus oxychloride (1 equiv.) was added dropwise under argon atmosphere to the reaction mixture, which was stirred at room temperature for 1 h. After the completion of the reaction, as monitored by TLC, the crude mixture was transferred into a column pre-packed with dry 100-200 mesh size silica, and the isocyanide was eluted with Et_2O.

4-isocyano-1,1'-biphenyl **1**. The title compound was prepared according to general procedure A. The crude material was purified by column chromatography (*n*-hexane/ethyl acetate 95:5) to give the product as an orange solid (97% yield). Characterization data are in agreement with literature reports.[48]

4'-isocyano-3-methoxy-1,1'-biphenyl **2**. The title compound was prepared according to general procedure B. The crude material was purified by column chromatography (*n*-hexane/ethyl acetate 9:1) to give the product as a green solid (85% yield). ^{1}H NMR (400 MHz, $CDCl_3$) δ 7.61 – 7.58 (m, 2H), 7.45 – 7.40 (m, 2H), 7.38 (t, J = 8.0 Hz, 1H), 7.15 – 7.13 (m, 1H), 7.08 – 7.07 (m, 1H), 6.95 – 6.93 (m, 1H), 3.87 (s, 3H); ^{13}C {^{1}H} NMR (101 MHz, $CDCl_3$) δ 164.6, 160.1, 142.3, 140.9, 130.1, 128.1, 126.8, 125.7 (t, J = 11.2 Hz), 119.6, 113.5, 113.0, 55.4; HRMS (ESI) *m/z*: calcd $[M + H]^+$ for $C_{14}H_{12}NO^+$ 210.0913; found $[M + H]^+$ 210.0908.

4'-isocyano-3-(trifluoromethyl)-1,1'-biphenyl **3**. The title compound was prepared according to general procedure B. The crude material was purified by column chromatography (*n*-hexane/ethyl acetate 9:1) to give the product as a green solid (71% yield); ^{1}H NMR (700 MHz, $CDCl_3$) δ 7.80 (s, 1H), 7.74 (d, J = 7.7 Hz, 1H), 7.66 (d, J = 7.7 Hz, 1H), 7.64 – 7.57 (m, 3H), 7.49 (d, J = 8.4 Hz, 2H); ^{13}C {^{1}H} NMR (101 MHz, $CDCl_3$) δ 165.3, 140.9, 140.2, 131.5 (q, ^2J(C,F) = 32.4 Hz), 130.4, 129.6, 128.2, 127.0, 126.3 (t, J = 11.6 Hz), 124.9 (q, ^3J(C,F) = 3.6 Hz), 124.0 (q, ^1J(C,F) = 273.2 Hz); 123.9 (q, ^3J = 3.6 Hz); HRMS (ESI) *m/z*: calcd $[M + H]^+$ for $C_{14}H_9F_3N^+$ 248.0682; found $[M + H]^+$ 248.0675.

4'-isocyano-[1,1'-biphenyl]-3-carbonitrile **4**. The title compound was prepared according to general procedure B. The crude material was purified by column chromatography (*n*-hexane/ethyl acetate 95:5) to give the product as a beige solid (89% yield); ^{1}H NMR (400 MHz, $CDCl_3$) δ 7.84 (s, 1H), 7.79 (d, J = 7.5 Hz, 1H), 7.69 (d, J = 7.2 Hz, 1H), 7.60 – 7.58 (m, 3H), 7.51 – 7.49 (m, 2H); ^{13}C {^{1}H} NMR (101 MHz, $CDCl_3$) δ 165.6, 140.6, 140.0, 131.6, 131.4, 130.7, 129.9, 128.1, 127.2, 126.6 (t, J = 13.2 Hz), 118.4, 113.4; HRMS (ESI) *m/z*: calcd $[M + H]^+$ for $C_{14}H_9N_2^+$ 205.0760; found $[M + H]^+$ 205.0757.

4'-isocyano-3-nitro-1,1'-biphenyl **5**. The title compound was prepared according to general procedure C to give the product as a brownish solid (51% yield). ^{1}H NMR (600 MHz, $CDCl_3$) δ 8.43 (s, 1H), 8.27 – 8.25 (m, 1H), 7.90 – 7.88 (m, 1H), 7.67 – 7.64 (m, 3H), 7.52 (d, J = 8.0 Hz, 2H); ^{13}C {^{1}H} NMR (101 MHz, $CDCl_3$) δ 165.8, 148.8, 141.0, 139.8, 133.0, 130.1, 128.3, 127.2, 126.7 (t, J = 11.9 Hz), 123.0, 122.0; HRMS (ESI) *m/z*: calcd $[M + H]^+$ for $C_{13}H_9N_2O_2^+$ 225.0659; found $[M + H]^+$ 225.0653.

1-isocyano-3-(trifluoromethyl)benzene **6**. The title compound was prepared according to general procedure D to give the product as a brown sticky solid (31% yield). Characterization data are in agreement with literature reports.[51]

3-isocyanobenzonitrile **7**. The title compound was prepared according to general procedure A. The crude material was purified by column chromatography (*n*-hexane/ethyl acetate 95:5) to give the product as a pale-yellow solid (88% yield). Characterization data are in agreement with literature reports.[52]

1-isocyano-3-nitrobenzene **8**. The title compound was prepared according to general procedure A. The crude material was purified by column chromatography (*n*-hexane/ethyl acetate 9:1) to give the product as a brownish solid (80% yield). Characterization data are in agreement with literature reports.[53]

1-isocyano-4-nitrobenzene **9**. The title compound was prepared according to general procedure A. The crude material was purified by column chromatography (*n*-hexane/ethyl acetate 9:1) to give the product as a brownish solid 85% yield). Characterization data are in agreement with literature reports.[53]

Synthesis of the Starting Materials. Procedure for the Synthesis of the Hantzsch ester 10. In a 50 mL round-bottom flask equipped with a magnetic stir bar 2-([1,1'-biphenyl]-4-yl)ethan-1-ol (200 mg, 1 mmol) was dissolved in CH_2Cl_2 (1 mL, 1 M) and PIDA (354.4 mg, 1.1 mmol, 1.1 equiv.) and TEMPO (15.6 mg, 0.1 mmol, 0.1 equiv.) were then added.[7] The mixture was stirred at room temperature for 2 h, until the completion of the reaction, as monitored by TLC. Then the solvent was removed under a positive flow of nitrogen and the crude reaction mixture was used in the next step without purification. The crude 2-([1,1'-biphenyl]-4-yl)acetaldehyde was dissolved in MeOH (670 µL, 1.5 M), and ethyl acetoacetate (255.2 µL, 2 mmol, 2 equiv.) and aqueous NH_4OH (NH_3 30-33% in water, 10 mmol, 10 equiv.) were added. The resulting mixture was stirred at reflux overnight, then the solvent was removed under vacuum and the crude material was purified by silica gel chromatography (*n*-hexane/ ethyl acetate 96:4) to give diethyl 4-([1,1'-biphenyl]-4-ylmethyl)-2,6-dimethyl-1,4-dihydropyridine-3,5-dicarboxylate **10** as a beige solid (213.8 mg, 51% yield). ^{1}H NMR (400 MHz, $CDCl_3$) δ 7.58 – 7.55 (m, 2H), 7.44 – 7.40 (m, 4H), 7.33 – 7.30 (m, 1H), 7.12 – 7.10 (m, 2H), 5.26 (br s, -N*H*), 4.22 (t, J = 5.5 Hz, 1H), 4.13 – 3.99 (m, 4H), 2.62 (d, J = 5.6 Hz, 2H), 2.20 (s, 6H), 1.23 (t, J = 7.1 Hz, 6H); ^{13}C {^{1}H} NMR (101 MHz, $CDCl_3$) δ 167.8, 145.3, 141.3, 138.6, 138.5, 130.5, 128.7, 127.0, 126.9, 126.0, 102.1, 59.6, 42.1, 35.6, 19.3, 14.4.; HRMS (ESI) *m/z*: calcd $[M + H]^+$ for $C_{26}H_{30}NO_4^+$ 420.2170; found $[M + H]^+$ 420.2169.

Procedure for the Synthesis of the potassium alkyltrifluoroborate 14.[54] To a 100 mL Schlenk tube equipped with a magnetic stir bar 4-(bromomethyl)-1,1'-biphenyl (500 mg, 2 mmol), CuI (38.1 mg, 0.2 mmol, 10 mol %), PPh_3 (68.2 mg, 0.26 mmol, 13 mol %), LiOMe (159.9 mg, 4 mmol, 2 equiv.), and bis(pinacolato)diboron (761.8 mg, 3 mmol, 1.5 equiv.) were added and the vessel was evacuated and filled with argon three times. Dry DMF (8 mL, 0.25 M) was added by syringe under argon atmosphere. The resulting reaction mixture was stirred vigorously at 25° C for 18 h. The reaction mixture was diluted with EtOAc and filtered through silica gel. Then the mixture was washed with saturated aqueous brine (x3). The organic layer was dried over sodium sulfate, filtered, concentrated to near dryness, then diluted with MeOH (8 mL) and cooled to 0 °C. Saturated aqueous solution of KHF_2 (5 mL, 782 mg, 10 mmol) was added dropwise and the resulting suspension was stirred for 2 h and then concentrated to dryness. The residue, a white solid, was extracted with hot acetone (3 x 6 mL), and the combined filtered extracts were concentrated to near dryness. Cold ether was added, and the resultant precipitate was collected and dried to afford potassium ([1,1'-biphenyl]-4-ylmethyl)trifluoroborate **14** as a white solid (274.5 mg, 50% yield). Characterization data are in agreement with literature reports.[55]

General Procedure for the Synthesis of *α*-ketoacids.[56] To a 25 mL dry round bottom flask equipped with a magnetic stir bar the aryl-ketone (1 equiv.) and selenium dioxide (2 equiv.) were added followed by anhydrous pyridine (0.25 M). The reaction mixture was then stirred at 110 °C for 16 hours. After completion of the reaction, as monitored by TLC, the solution containing precipitated selenium was filtered and the residue was washed with EtOAc. The filtrate was treated with 1 M aqueous NaOH and the aqueous layer was separated. This procedure was repeated 3 times and the aqueous layers were combined, then acidified with 1 M aqueous HCl (until pH ~ 1.5). Thus, the mixture was extracted with EtOAc (x3), and the combined organic layers were washed with brine, dried over sodium sulfate, and concentrated under reduced pressure to provide a solid, which was washed three times with *n*-hexane and then dried to afford the desired *α*-ketoacid.

2-([1,1'-biphenyl]-4-yl)-2-oxoacetic acid. The title compound was prepared according to the reported general procedure (off-white solid, 66% yield). Characterization data are in agreement with literature reports.[57]

2-(2,4-dichlorophenyl)-2-oxoacetic acid. The title compound was prepared according to the reported general procedure (reddish solid, 80% yield). Characterization data are in agreement with literature reports.[58]

2-(benzo[d][1,3]dioxol-5-yl)-2-oxoacetic acid. The title compound was prepared according to the reported general procedure (off-white solid, 79% yield). Characterization data are in agreement with literature reports.[57]

2-oxo-2-(4-phenoxyphenyl)acetic acid. The title compound was prepared according to the reported general procedure (yellowish oil, 81% yield). Characterization data are in agreement with literature reports.[59]

2-(naphthalen-2-yl)-2-oxoacetic acid. The title compound was prepared according to the reported general procedure (yellow solid, 85% yield). Characterization data are in agreement with literature reports.[57]

General Procedure for the synthetic studies involving Hantzsch esters. In a 4 mL colorless screw-cap glass vial

equipped with a magnetic stir bar diethyl 4-([1,1'-biphenyl]-4-ylmethyl)-2,6-dimethyl-1,4-dihydropyridine-3,5-dicarboxylate **10** (33.6 mg, 0.08 mmol) was dissolved in dry CH_3CN (530 µL, 0.15 M), and the selected H-donor (HE or TIS, 0.08 mmol, 1 equiv.) and isocyanide (0.016 mmol, 20 mol %) were then added. The resulting mixture was stirred open flask in a PhotoRedOx Box (EvoluChem™), under 30 W or 1 W blue LEDs irradiation, at room temperature, for 20 h or 48 h. Then the crude material was diluted with EtOAc and washed with an aqueous solution of 1 M HCl (x3). The aqueous layers were further extracted with EtOAc (x2), then the combined organic extracts were washed with brine, dried over sodium sulfate, filtered, and concentrated under vacuum. The crude material was purified by silica gel chromatography.

4-(hydroperoxymethyl)-1,1'-biphenyl **13**. The title compound was prepared according to the reported general procedure, employing 1-isocyano-3-nitrobenzene **8** (2.4 mg, 0.016 mmol, 20 mol %), TIS as the H-donor (16.4 µL 0.08 mmol, 1 equiv.), and 30 W blue LEDs as the light source, with a reaction time of 48 h. The crude material was purified by column chromatography (*n*-hexane/ ethyl acetate 99:1) to give the product as a pale-yellow solid (9.3 mg, 58 % yield); ^{1}H NMR (400 MHz, $CDCl_3$) δ 8.02 (br s, -OO*H*), 7.63 – 7.58 (m, 4H), 7.49 – 7.43 (m, 4H), 7.39 – 7.34 (m, 1H), 5.06 (s, 2H); ^{13}C {^{1}H} NMR (101 MHz, $CDCl_3$) δ 141.6, 140.7, 134.7, 129.5, 128.8, 127.5, 127.4, 127.2, 79.0; HRMS (ESI) *m/z*: calcd $[M + H]^+$ for $C_{13}H_{13}O_2^+$ 201.0910; found $[M + H]^+$ 201.0902; *m/z* of the corresponding aldehyde is also present: calcd $[M + H]^+$ for $C_{13}H_{11}O^+$ 183.0805; found $[M + H]^+$ 183.0805.

General Procedure for the synthetic studies involving potassium alkyltrifluoroborates. In a 4 mL colorless screw-cap glass vial equipped with a magnetic stir bar potassium ([1,1'-biphenyl]-4-ylmethyl)trifluoroborate **14** (21.9 mg, 0.08 mmol) was dissolved in a CH_3CN/H_2O mixture (9:1, 8:2 or 3:1, 530 µL, 0.15 M) and the selected H-donor (HE or TIS, 0.08 mmol, 1 equiv.) and isocyanide (0.016 mmol, 20 mol %) were then added. The resulting mixture was stirred open flask in a PhotoRedOx Box (EvoluChem™), under 30 W blue LEDs irradiation, at room temperature, for 20 h or 48 h. Then the solvent was removed under vacuum and the crude material was purified by silica gel chromatography.

[1,1'-biphenyl]-4-ylmethanol **15**. The title compound was prepared according to the reported general procedure, employing 1-isocyano-3-nitrobenzene **8** (2.4 mg, 0.016 mmol, 20 mol %), TIS as the H-donor (16.4 µL 0.08 mmol, 1 equiv.), and an 8:2 CH_3CN/H_2O mixture as the solvent system, with a reaction time of 20 h. The crude material was purified by column chromatography (*n*-hexane/ ethyl acetate 98:2) to give the product as a pale-yellow solid (9.6 mg, 65% yield). Characterization data are in agreement with literature reports.[60]

Synthetic studies involving *α*-ketoacids. General Procedure for the Preparation of aldehydes 20-24. In a 4 mL colorless screw-cap glass vial equipped with a magnetic stir bar the *α*-ketoacid (0.08 mmol) was dissolved in a 3:1 CH_3CN/H_2O mixture (320 µL, 0.25 M,) and K_2HPO_4 (16.7 mg, 0.096 mmol, 1.2 equiv.), TIS (16.4 µL 0.08 mmol, 1 equiv.) and 3-isocyanobenzonitrile **7** (2.1 mg, 20 mol %) were then added. The resulting mixture was stirred in a PhotoRedOx Box (EvoluChem™), under 30 W blue LEDs irradiation, at room temperature, for 72 h. Then the solvent was removed under vacuum and the crude material was purified by silica gel chromatography.

[1,1'-biphenyl]-4-carbaldehyde **20**. The title compound was prepared according to the reported general procedure. The crude material was purified by column chromatography (*n*-hexane/ ethyl acetate 99:1) to give the product as a colorless oil (12.0 mg, 82 % yield). Characterization data are in agreement with literature reports.[61]

2,4-dichlorobenzaldehyde **21**. The title compound was prepared according to the reported general procedure. The crude material was purified by column chromatography (*n*-hexane/ ethyl acetate 99.5:0.5) to give the product as a colorless oil (9.0 mg, 64 % yield). Characterization data are in agreement with literature reports.[61]

benzo[d][1,3]dioxole-5-carbaldehyde **22**. The title compound was prepared according to the reported general procedure. The crude material was purified by column chromatography (*n*-hexane/ ethyl acetate 99:1) to give the product as a colorless oil (4.5 mg, 37 % yield). Characterization data are in agreement with literature reports.[62]

4-phenoxybenzaldehyde **23**. The title compound was prepared according to the reported general procedure. The crude material was purified by column chromatography (*n*-hexane/ ethyl acetate 99.5:0.5) to give the product as a colorless oil (8.4 mg, 53 % yield). Characterization data are in agreement with literature reports.[63]

2-naphthaldehyde **24**. The title compound was prepared according to the reported general procedure. The crude material was purified by column chromatography (*n*-hexane/ ethyl acetate 99.5:0.5) to give the product as a colorless oil (5.6 mg, 45 % yield). Characterization data are in agreement with literature reports.[61]

General Procedure for the tandem one-pot Passerini 3-CR. In a 4 mL colorless screw-cap glass vial equipped with a magnetic stir bar the *α*-ketoacid (0.08 mmol) was dissolved in a 3:1 CH_3CN/H_2O mixture (320 µL, 0.25 M) and K_2HPO_4 (16.7 mg, 0.096 mmol, 1.2 equiv.), TIS (16.4 µL 0.08 mmol, 1 equiv.) and 3-isocyanobenzonitrile **7** (2.1 mg, 20 mol %) were then added. The resulting mixture was stirred in a PhotoRedOx Box (EvoluChem™), under 30 W blue LEDs irradiation, at room temperature, for 20 h. Then the selected isocyanide (0.16 mmol, 2 equiv.) and carboxylic acid (0.24 mmol, 3 equiv.) were added *in situ,* and the resulting mixture was stirred under 30 W blue LEDs irradiation, at room temperature, for additional 72 h. The crude material was diluted with EtOAc and washed with a saturated aqueous solution of $NaHCO_3$ (x3). The aqueous layers were further extracted with EtOAc (x2), then the combined organic extracts were washed with brine, dried over sodium sulfate, filtered, and concentrated under vacuum. The crude material was purified by silica gel chromatography.

2-(tert-butylamino)-2-oxo-1-phenylethyl 3-methylbenzoate **25**. The title compound was prepared according to the reported general procedure. The crude material was purified by column chromatography (*n*-hexane/ ethyl acetate 96:4) to give the product as a white solid (15.1 mg, 58 % yield). ^{1}H NMR (400 MHz, $CDCl_3$) δ 7.89 – 7.88 (m, 2H), 7.54 – 7.52 (m, 2H), 7.43 – 7.33 (m, 5H), 6.21 (s, 1H), 6.00 (br s -N*H*), 2.42 (s, 3H), 1.37 (s, 9H); ^{13}C {^{1}H} NMR (101 MHz, $CDCl_3$) δ 167.4, 165.1, 138.5, 136.0, 134.4, 130.3, 128.9, 128.8, 128.5, 127.5, 126.9, 76.0, 51.6, 28.7, 21.3;

HRMS *m/z*: calcd $[M + H]^+$ for $C_{20}H_{24}NO_3^+$ 326.1751; found $[M + H]^+$ 326.1737.

1-([1,1'-biphenyl]-4-yl)-2-(cyclohexylamino)-2-oxoethyl-4-methoxybenzoate **26**. The title compound was prepared according to the reported general procedure. The crude material was purified by column chromatography (*n*-hexane/ ethyl acetate 9:1) to give the product as a white solid (14.1 mg, 40 % yield). ^{1}H NMR (400 MHz, $CDCl_3$) δ 8.07 (d, *J* = 8.8 Hz, 2H), 7.62 – 7.56 (m, 6H), 7.43 (t, J = 7.6 Hz, 2H), 7.37 – 7.3 (m, 1H), 6.97 (d, *J* = 8.8 Hz, 2H), 6.33 (s, 1H), 6.11 (br d, *J* = 8.1 Hz, -N*H*), 3.91 – 3.80 (m, 4H), 1.97 – 1.90 (m, 2H), 1.72 - 1.66 (m, 2H), 1.43 – 1.32 (m, 2H), 1.22 – 1.13 (m, 4H); ^{13}C {^{1}H} NMR (101 MHz, $CDCl_3$) δ 167.5, 164.6, 1634.0, 141.8, 140.6, 135.0, 131.9, 128.8, 127.8, 127.5 (3C) , 127.2, 121.6, 114.0, 75.4, 55.5, 48.2, 33.0, 32.9, 25.5, 24.7, 24.7; HRMS *m/z:* calcd $[M + H]^+$ for $C_{28}H_{30}NO_4^+$ 444.2169; found $[M + H]^+$ 444.2154.

2-(tert-butylamino)-2-oxo-1-phenylethyl(4R)-4-((3R,5S,7R,8R,9S,10S,12S,13R,14S,17R)-3,7,12-trihydroxy-10,13-dimethylhexadecahydro-1H-cyclopenta[a]phenanthren-17-yl)pentanoate **27**. The title compound was prepared according to the reported general procedure. The crude material was purified by column chromatography (dichloromethane/ methanol 96:4) to give the product as a pale-yellow solid (15.1 mg, 32 % yield). ^{1}H NMR (400 MHz, $CDCl_3$) δ 7.41 – 7.33 (m, 5H), 5.96 (s, 1H), 5.92 (br s, -N*H*), 3.96 (br s, 1H), 3.84 (br s, 1H), 3.48 – 3.41 (m, 1H), 2.53 – 2.32 (m, 1H), 2.24 – 2.16 (m, 2H), 1.96 – 1.51 (m, 10H), 1.44 – 1.32 (m, 14H), 1.30 – 1.18 (m, 4H), 1.14 – 1.06 (m, 1H), 1.00 – 0.94 (m, 4H), 0.92 – 0.85 (m, 6H), 0.64 (s, 3H)*;* ^{13}C NMR {^{1}H} (101 MHz, $CDCl_3$, rotamers) δ 172.4, 172.3, 167.5, 167.4, 136.1, 136.1, 128.8, 128.8, 128.7, 127.5, 127.4, 75.5, 75.5, 73.0, 72.0, 68.4, 51.5, 46.9, 46.5, 41.9, 41.4, 39.6, 39.5, 35.2, 35.1, 35.0, 34.7, 34.6, 31.6, 31.2, 31.2, 30.8, 30.7, 30.4, 29.9, 29.7, 28.7, 28.3, 27.5, 27.4, 26.6, 23.2, 22.7, 22.5, 17.3, 14.1, 12.5; HRMS *m/z*: calcd $[M + H]^+$ for $C_{36}H_{56}NO_6^+$ 598.4103; found $[M + H]^+$ 598.4083.

2-(cyclohexylamino)-2-oxo-1-phenylethyl-5-(2,5-dimethylphenoxy)-2,2-dimethylpentanoate **28**. The title compound was prepared according to the reported general procedure. The crude material was purified by column chromatography (*n*-hexane/ ethyl acetate 97:3) to give the product as a colorless sticky solid (8.6 mg, 23 % yield). ^{1}H NMR (400 MHz, $CDCl_3$) δ 7.43 – 7.41 (m, 2H), 7.37 – 7.33 (m, 3H), 6.99 (d, *J* = 7.4 Hz, 1H), 6.66 (d, J = 7.4 Hz, 1H), 6.58 (s, 1H), 6.05 (s, 1H), 5.95 (br d, *J* = 7.7 Hz, -N*H*), 3.91 – 3.78 (m, 3H), 2.30 (s, 3H), 2.14 (s, 3H), 1.94 – 1.58 (m, 6H), 1.43 – 1.26 (m, 9H), 1.16 – 1.05 (m, 2H), 0.93 – 0.82 (m, 3H); ^{13}C {^{1}H} NMR (101 MHz, $CDCl_3$) δ 175.8, 167.4, 161.6, 136.5, 135.9, 130.3, 128.8, 128.7, 127.2, 123.5, 120.8, 112.0, 75.3, 67.8, 48.0, 42.2, 37.1, 32.9, 32.9, 29.7, 25.4, 25.3, 25.1, 25.0, 24.6, 21.4, 15.8; HRMS *m/z*: calcd $[M + H]^+$ for $C_{29}H_{40}NO_4^+$ 466.2952; found $[M + H]^+$ 466.2934.

General Procedure for the tandem one-pot Strecker 3-CR. In a 4 mL colorless screw-cap glass vial equipped with a magnetic stir bar the *α*-ketoacid (0.08 mmol) was dissolved in a 3:1 CH_3CN/H_2O mixture (320 µL, 0.25 M) and K_2HPO_4 (16.7 mg, 0.096 mmol, 1.2 equiv.), TIS (16.4 µL 0.08 mmol, 1 equiv.) and 3-isocyanobenzonitrile ***7*** (2.1 mg, 20 mol %) were then added. The resulting mixture was stirred in a PhotoRedOx Box (EvoluChem™), under 30 W blue LEDs irradiation, at room temperature, for 48 h. Then a secondary amine (0.08 mmol, 1 equiv.) and TMSCN (20 µL, 0.16 mmol, 2 equiv.) were added *in situ,* and the resulting mixture was stirred under 30 W blue LEDs irradiation, at room temperature, for additional 48 h. The crude material was diluted with EtOAc and washed with a saturated aqueous solution of $NaHCO_3$ (x3). The aqueous layers were further extracted with EtOAc (x2), then the combined organic extracts were washed with brine, dried over sodium sulfate, filtered, and concentrated under vacuum. The crude material was purified by silica gel chromatography.

2-(benzyl(methyl)amino)-2-phenylacetonitrile **29**. The title compound was prepared according to the reported general procedure. The crude material was purified by column chromatography (*n*-hexane/ ethyl acetate 99:1) to give the product as a colorless oil (11.5 mg, 61 % yield). Characterization data are in agreement with literature reports.[64]

2-morpholino-2-phenylacetonitrile **30**. The title compound was prepared according to the reported general procedure. The crude material was purified by column chromatography (*n*-hexane/ ethyl acetate 97:3) to give the product as a white solid (10.2 mg, 63 % yield). Characterization data are in agreement with literature reports.[65]

2-([1,1'-biphenyl]-4-yl)-2-(piperidin-1-yl)acetonitrile **31**. The title compound was prepared according to the reported general procedure. The crude material was purified by column chromatography (*n*-hexane/ ethyl acetate 99:1) to give the product as a pale-yellow solid (16.4 mg, 74 % yield). ^{1}H NMR (400 MHz, $CDCl_3$) δ 7.65 – 7.57 (m, 6H), 7.45 (t, *J* = 7.6 Hz, 2H), 7.39 – 7.35 (m, 1H), 4.86 (s, 1H), 2.61 – 2.51 (m, 4H), 1.67 – 1.59 (m, 4H), 1.53 – 1-49 (m, 2H); ^{13}C {^{1}H} NMR (101 MHz, $CDCl_3$) δ 141.7, 140.3 (2C), 128.9, 128.3, 127.6, 127.4, 127.1, 115.6, 62.8, 51.0, 25.8, 23.9; HRMS *m/z*: calcd $[M + H]^+$ for $C_{19}H_{21}N_2^+$ 277.1699; found $[M + H]^+$ 277.1691.

Procedure for the tandem one-pot Ugi-Tetrazole 4-CR. *1-((1-cyclohexyl-1H-tetrazol-5-yl)(phenyl)methyl)piperidine* **32**. In a 4 mL colorless screw-cap glass vial equipped with a magnetic stir bar phenylglyoxylic acid **16** (12.0 mg, 0.08 mmol) was dissolved in a 9:1 CH_3CN/H_2O mixture (320 µL, 0.25 M) and K_2HPO_4 (16.7 mg, 0.096 mmol, 1.2 equiv.), TIS (16.4 µL 0.08 mmol, 1 equiv.) and 3-isocyanobenzonitrile **7** (2.1 mg, 20 mol %) were then added. The resulting mixture was stirred in a PhotoRedOx Box (EvoluChem™), under 30 W blue LEDs irradiation, at room temperature, for 48 h. Then cyclohexyl isocyanide (19.6 µL, 0.16 mmol, 2 equiv.), $TMSN_3$ (21.1 µL, 0.16 mmol, 2 equiv.) and piperidine (11.9 µL, 0.12 mmol, 1.5 equiv.) were added *in situ,* and the resulting mixture was stirred under 30 W blue LEDs irradiation, at room temperature, for additional 48 h. Then the solvent was removed under vacuum and the crude material was purified by silica gel chromatography (*n*-hexane/ ethyl acetate 97:3) to give the product as a colorless oil (13.2 mg, 51 % yield). ^{1}H NMR (400 MHz, $CDCl_3$) δ 7.43 (d, *J* = 7.6 Hz, 2H), 7.36 – 7.26 (m, 3H), 5.00 (s, 1H), 4.68 (m, 1H), 2.60 – 2.53 (m, 2H), 2.29 – 2.21 (m, 2H), 2.01 – 1.72 (m, 7H), 1.63 – 1.44 (m, 6H), 1.38 – 1.25 (m, 3H); ^{13}C {^{1}H} NMR (101 MHz, $CDCl_3$) δ 153.7, 135.7, 128.6, 128.5, 128.3, 65.7, 58.0, 52.6, 32.8, 32.8, 26.1, 25.6, 25.4,

24.9, 24.2; HRMS *m/z*: calcd $[M + H]^+$ for $C_{19}H_{28}N_5^+$ 326.2340; found $[M + H]^+$ 326.2327.

Procedure for the Passerini 3-CR starting from benzaldehyde. In a 4 mL colorless screw-cap glass vial equipped with a magnetic stir bar benzaldehyde (8.2 µL, 0.08 mmol), *tert*-butyl isocyanide (9.0 µL, 0.08 mmol, 1 equiv.) and *m*-toluic acid (10.9 mg, 0.08 mmol, 1 equiv.) were dissolved in a 3:1 CH_3CN/H_2O mixture (320 µL, 0.25 M). The reaction was stirred at room temperature for 72 h, then the solvent was removed under vacuum and the yield determined by NMR analysis of the crude reaction mixture after adding 1,3,5-trimethoxybenzene as internal standard (58 % NMR yield).

Procedure for the Strecker 3-CR starting from benzaldehyde. In a 4 mL colorless screw-cap glass vial equipped with a magnetic stir bar benzaldehyde (8.2 µL, 0.08 mmol), *N*-benzylmethylamine (10.3 µL, 0.08 mmol, 1 equiv.) and TMSCN (20.0 µL, 0.16 mmol, 2 equiv.) were dissolved in a 3:1 CH_3CN/H_2O mixture (320 µL, 0.25 M). The reaction was stirred at room temperature for 48 h, then the solvent was removed under vacuum and the yield determined by NMR analysis of the crude reaction mixture after adding 1,3,5-trimethoxybenzene as internal standard (85 % NMR yield).

Procedure for the Ugi-tetrazole 4-CR starting from benzaldehyde. In a 4 mL colorless screw-cap glass vial equipped with a magnetic stir bar benzaldehyde (8.2 µL, 0.08 mmol), cyclohexyl isocyanide (9.9 µL, 0.08 mmol, 1 equiv.), $TMSN_3$ (10.1 µL, 0.08 mmol, 1 equiv.) and piperidine (7.9 µL, 0.08 mmol, 1 equiv.) were dissolved in a 9:1 CH_3CN/H_2O mixture (320 µL, 0.25 M). The reaction was stirred at room temperature for 48 h, then the solvent was removed under vacuum and the yield determined by NMR analysis of the crude reaction mixture after adding 1,3,5-trimethoxybenzene as internal standard (63 % NMR yield).

Deuterium labelling experiments. General Procedure for the Preparation of deuterium labeled aldehydes 20-*D*, 21-*D*, and 24-*D*. In a 4 mL colorless screw-cap glass vial equipped with a magnetic stir bar the *α*-ketoacid (0.08 mmol) was dissolved in a 3:1 CH_3CN/D_2O mixture (320 µL, 0.25 M) and K_2HPO_4 (16.7 mg, 0.096 mmol, 1.2 equiv.), TIS (16.4 µL 0.08 mmol, 1 equiv.) and 3-isocyanobenzonitrile **7** (2.1 mg, 20 mol %) were then added. The resulting mixture was stirred in a PhotoRedOx Box (EvoluChem™), under 30 W blue LEDs irradiation, at room temperature, for 72 h. Then the solvent was removed under vacuum and the crude material was purified by silica gel chromatography.

[1,1'-biphenyl]-4-carbaldehyde-d **20-*D***. The title compound was prepared according to the reported general procedure. The crude material was purified by column chromatography (*n*-hexane/ ethyl acetate 99:1) to give the product as a colorless oil (12.8 mg, 87 % yield, 98 % deuteration Characterization data are in agreement with literature reports.[66]

2,4-dichlorobenzaldehyde-d **21-*D***. The title compound was prepared according to the reported general procedure. The crude material was purified by column chromatography (*n*-hexane/ ethyl acetate 99.5:0.5) to give the product as a colorless oil (7.0 mg, 50 % yield, 97 % deuteration). ^{1}H NMR (400 MHz, $CDCl_3$) *δ* 7.88 (d, *J* = 8.4 Hz, 1H), 7.49 (d, *J* = 1.9 Hz, 1H), 7.38 (dd, *J* = 8.4, 1.9 Hz, 2H); ^{13}C {^{1}H} NMR (101 MHz, $CDCl_3$) *δ* 188.2 (t, *J* = 28.4 Hz), 141.1, 138.6, 130.9 (t, *J* = 3.3 Hz), 130.5, 130.3, 128.0; HRMS *m/z*: calcd $[M + H]^+$ for $C_7H_4DCl_2O^+$ 175.9775; found $[M + H]^+$ 175.9771.

2-naphthaldehyde-d **24-*D***. The title compound was prepared according to the reported general procedure. The crude material was purified by column chromatography (*n*-hexane/ ethyl acetate 99.5:0.5) to give the product as a colorless oil (4.9 mg, 39 % yield, 97 % deuteration). Characterization data are in agreement with literature reports.[66]

Procedure for the tandem one-pot Passerini 3-CR to D-labelled derivative 33-*D*. *1-([1,1'-biphenyl]-4-yl)-2-(tert-butylamino)-2-oxoethyl-1-d-3-methylbenzoate* **33-*D***. In a 4 mL colorless screw-cap glass vial equipped with a magnetic stir bar 2-([1,1'-biphenyl]-4-yl)-2-oxoacetic acid **19** (18.1 mg, 0.08 mmol) was dissolved in a 3:1 CH_3CN/D_2O mixture (320 µL, 0.25 M) and K_2HPO_4 (16.7 mg, 0.096 mmol, 1.2 equiv.), TIS (16.4 µL 0.08 mmol, 1 equiv.) and 3-isocyanobenzonitrile **7** (2.1 mg, 20 mol %) were then added. The resulting mixture was stirred in a PhotoRedOx Box (EvoluChem™), under 30 W blue LEDs irradiation, at room temperature, for 20 h. Then *tert*-butyl isocyanide (18 µL, 0.16 mmol, 2 equiv.) and *m*-toluic acid (32.7 mg, 0.24 mmol, 3 equiv.) were added *in situ,* and the resulting mixture was stirred under 30 W blue LEDs irradiation, at room temperature, for additional 72 h. The crude material was diluted with EtOAc and washed with a saturated aqueous solution of $NaHCO_3$ (x3). The aqueous layers were further extracted with EtOAc (x2), then the combined organic extracts were washed with brine, dried over sodium sulfate, filtered, and concentrated under vacuum. The crude material was purified by silica gel chromatography (*n*-hexane/ethyl acetate 96:4) to give the product as a yellow solid (16.1 mg, 50 % yield, 100 % deuteration). ^{1}H NMR (400 MHz, $CDCl_3$) *δ* 7.91 – 7.90 (m, 2H), 7.63 – 7.57 (m, 6H), 7.46 – 7.33 (m, 5H), 6.07 (br s, -N*H*), 2.43 (s, 3H), 1.39 (s, 9H); ^{13}C {^{1}H} NMR (101 MHz, $CDCl_3$) *δ* 167.4, 165.1, 141.8, 140.6, 138.6, 134.9, 134.4, 130.3, 129.3, 128.8, 128.6, 127.9, 127.6, 127.5, 127.2, 126.9, 75.5 (t, J = 23.2 Hz), 51.6, 28.7, 21.3; HRMS *m/z*: calcd $[M + H]^+$ for $C_{26}H_{27}DNO_3^+$ 403.2127; found $[M + H]^+$ 403.2115.

Procedure for the tandem one-pot Strecker 3-CR to D-labelled derivative 29-*D*. *2-(benzyl(methyl)amino)-2-phenylacetonitrile-d* **29-*D***. In a 4 mL colorless screw-cap glass vial equipped with a magnetic stir bar phenylglyoxylic acid **16** (12.0 mg, 0.08 mmol) was dissolved in a 3:1 CH_3CN/D_2O mixture (0.25 M, 320 µL) and K_2HPO_4 (16.7 mg, 0.096 mmol, 1.2 equiv.), TIS (16.4 µL 0.08 mmol, 1 equiv.) and 3-isocyanobenzonitrile **7** (2.1 mg, 20 mol %) were then added. The resulting mixture was stirred in a PhotoRedOx Box (EvoluChem™), under 30 W blue LEDs irradiation, at room temperature, for 48 h. Then *N*-benzylmethylamine (10.3 µL, 0.08 mmol, 1 equiv.) and TMSCN (20 µL, 0.16 mmol, 2 equiv.) were added *in situ,* and the resulting mixture was stirred under 30 W blue LEDs irradiation, at room temperature, for additional 48 h. The crude material was diluted with EtOAc and washed with a saturated aqueous solution of $NaHCO_3$ (x3). The aqueous layers were further extracted with EtOAc (x2), then the combined organic extracts were washed with brine, dried over sodium sulfate, filtered, and concentrated under vacuum. The crude material was purified by silica gel

chromatography (*n*-hexane/ ethyl acetate 99.5:0.5) to give the product as a colorless oil (9.6 mg, 51 % yield, 80 % deuteration). ^{1}H NMR (400 MHz, $CDCl_3$) δ 7.55 – 7.52 (m, 2H), 7.42 – 7.28 (m, 8H), 3.83 (d, J = 13.1 Hz, 1H), 3.56 (d, J = 13.1 Hz, 1H), 2.26 (s, 3H); ^{13}C {^{1}H} NMR (101 MHz, $CDCl_3$) δ 137.5, 133.8, 128.9, 128.8, 128.8, 128.7, 127.7, 127.7, 115.2, 59.8 (t, J = 22.2 Hz), 59.3, 38.3; HRMS *m/z*: calcd $[M + H]^+$ for $C_{16}H_{16}DN_2^+$ 238.1450; found $[M + H]^+$ 238.1440.

Procedure for the tandem one-pot Ugi-Tetrazole 4-CR to D-labelled derivative 32-*D*. *1-((1-cyclohexyl-1H-tetrazol-5-yl)(phenyl)methyl-d)piperidine* **32-*D***. In a 4 mL colorless screw-cap glass vial equipped with a magnetic stir bar phenylglyoxylic acid **16** (12.0 mg, 0.08 mmol) was dissolved in a 9:1 CH_3CN/D_2O mixture (320 µL, 0.25 M) and K_2HPO_4 (16.7 mg, 0.096 mmol, 1.2 equiv.), TIS (16.4 µL 0.08 mmol, 1 equiv.) and 3-isocyanobenzonitrile ***7*** (2.1 mg, 20 mol %) were then added. The resulting mixture was stirred in a PhotoRedOx Box (EvoluChem™), under 30 W blue LEDs irradiation, at room temperature, for 48 h. Then cyclohexyl isocyanide (19.6 µL, 0.16 mmol, 2 equiv.), $TMSN_3$ (21.1 µL, 0.16 mmol, 2 equiv.) and piperidine (11.9 µL, 0.12 mmol, 1.5 equiv.) were added *in situ,* and the resulting mixture was stirred under 30 W blue LEDs irradiation, at room temperature, for additional 48 h. Then the solvent was removed under vacuum and the crude material was purified by silica gel chromatography (*n*-hexane/ ethyl acetate 98:2) to give the product as a colorless oil (11.2 mg, 43 % yield, 93% deuteration). ^{1}H NMR (400 MHz, $CDCl_3$) δ 7.44 – 7.42 (m, 2H), 7.36 – 7.26 (m, 3H), 4.71 – 4.63 (m, 1H), 2.61 – 2.53 (m, 2H), 2.30 – 2.23 (m, 2H), 1.99 – 1.72 (m, 7H), 1.66 – 1.29 (m, 9H); ^{13}C NMR {^{1}H} (101 MHz, $CDCl_3$) δ 153.5, 135.5, 128.6, 128.6, 128.3, 65.2 (t, J = 19.8 Hz), 58.0, 52.5, 32.8, 32.8, 26.1, 25.6, 25.4, 24.9, 24.2; HRMS *m/z*: calcd $[M + H]^+$ for $C_{19}H_{27}DN_5^+$ 327.2402; found $[M + H]^+$ 327.2389.

Procedure for the Passerini 3-CR starting from *[1,1'-biphenyl]-4-carbaldehyde-d* 20-*D*. In a 4 mL colorless screw-cap glass vial equipped with a magnetic stir bar [1,1'-biphenyl]-4-carbaldehyde-d **20-*D*** (14.7 mg, 0.08 mmol), *tert*-butyl isocyanide (9.0 µL, 0.08 mmol, 1 equiv.) and *m*-toluic acid (10.9 mg, 0.08 mmol, 1 equiv.) were dissolved in a 3:1 CH_3CN/H_2O mixture (320 µL, 0.25 M). The reaction was stirred at room temperature for 72 h, then the crude material was diluted with EtOAc and washed with a saturated aqueous solution of $NaHCO_3$ (x3). The aqueous layers were further extracted with EtOAc (x2), then the combined organic extracts were washed with brine, dried over sodium sulfate, filtered, and concentrated under vacuum. The crude material was purified by silica gel chromatography (*n*-hexane/ethyl acetate 96:4) to give the product as a yellow solid (17.4 mg, 54 % yield).

Computational Methods. All the isocyanide compounds (**1**-**9**) were modeled by employing the Density Functional Theory (DFT) and its time-dependent (TD-DFT)[15–18] version to properly describe both the ground (S_0) and first singlet (S_1) excited electronic state properties, respectively. The global hybrid B3LYP[67–69] functional including the Grimme's dispersion correction (B3LYP-D3) combined with the 6-31+G(d,p) basis set was used for all the calculations. Calculations in acetonitrile were performed by using an implicit solvent model. All the calculations were performed by using the A.03 version of the commercial version of the Gaussian 16 suite of programs.[70] For more details see Supporting Information.

Cyclic voltammetry. Cyclic voltammograms were recorded on a Metrohm Autolab PGSTAT101. The experiments were performed using a glassy carbon working electrode and a saturated calomel (SCE) reference electrode. Scan rate 0.1 V/s. Compounds **1**-**9** and controls (biphenyl and 3,4-difluoro-nitrobenzene) were dissolved in distilled acetonitrile at ~ 1 mM concentration. Tetrabutylammonium tetrafluoroborate (TBATFB) (0.1 M) was used as the supporting electrolyte for cyclic voltammetry experiments in aqueous solution. The $E_{1/2}$ values were determined by an arithmetic average, $E_{1/2} = (E_{pc} + E_{pa})/2$ where E_{pc} and E_{pa} are the reduction and oxidation peak potentials.

UV-VIS spectroscopic measurements. UV-VIS spectra were acquired on a Jasco J-730 UV-VIS spectrophotometer (Jasco, Japan) equipped with an ETCS-761 Peltier temperature controller. Measurements were performed at 20 °C in a sealed quartz cuvette with a path length of 1 cm, using 100 nm/min scan rate, and the 220-600 nm wavelength range. All investigated compounds were dissolved in the CH_3CN/H_2O (8:2) solution, except in the case of **16** for which an CH_3CN/H_2O (3:1) solution was used. Compounds' solutions were used at 10 mM in all cases, except for **10** (200 mM).

Fluorescence experiments. Fluorescence spectra were performed at 20 °C on a FP-8300 spectrofluorometer (Jasco, Japan) equipped with a Peltier temperature controller system (Jasco PCT-818). A sealed quartz cuvette with a path length of 1 cm was used. Excitation wavelengths were set at the maximum of the absorption band of each investigated compound, i.e., 305 nm for **8**, 310 nm for **7**, 343 nm for **10**, and 350 nm for **16**. All investigated compounds were dissolved in CH_3CN/H_2O (8:2) solution, except in the case of **16** for which CH_3CN/H_2O (3:1) solution was used. Compounds' solutions were used at 10 mM in all cases, with the exception of **10** (200 mM) and **14** (100 mM). Stern-Volmer quenching of **7** (Fig. 5) was carried out by stepwise addition of **16** (0.1, 0.2, 0.4, 0.8 and 1.0 mol equiv.) to the cell containing a fixed concentration of **7** (10 mM) in CH_3CN/H_2O (8:2). Fluorescence emission spectra were recorded at 20 °C in the 320-650 nm wavelength range, using 100 nm/min scan speed, upon excitation at 310 nm. Both excitation and emission slit widths were set at 5 nm.

Supporting Information

The authors have cited additional references within the Supporting Information.[71-79]

Acknowledgements

Financial support from Università degli Studi di Napoli "Federico II", Napoli, Italy is acknowledged.

Keywords: Deuterium labelling • isocyanides • multicomponent reactions • Passerini reaction • visible-light photocatalysis

References

[1] Ugi, Isonitrile Chemistry, Academic Press, New York- London, 1971.

[2] V. G. Nenajdenko, *Isocyanide Chemistry: Applications in Synthesis and Material Science*, Wiley-VCH, **2012**.

[3] G. dos P. Gomes, Y. Loginova, S. Z. Vatsadze and I. V. Alabugin, *J. Am. Chem. Soc.* **2018**, *140*, 14272-14288.

[4] M. Giustiniano, E. Novellino, G. C. Tron, *Synthesis* **2016**, *48*, 2721-2731.

[5] A. Dömling, I. Ugi, *Angew. Chem. Int. Ed.* **2000**, *39*, 3168–3210.

[6] M. Giustiniano, A. Basso, V. Mercalli, A. Massarotti, E. Novellino, G. C. Tron, J. Zhu, *Chem. Soc. Rev.* **2017**, *46*, 1295-1357.

[7] C. Stephenson, T. Yoon, D. W. C. MacMillan, *Visible Light Photocatalysis in Organic Chemistry*, Wiley-VCH Verlag GmbH & Co. KGaA, Weinheim, Germany, **2018**.

[8] M. H. Shaw, J. Twilton, D. W. C. MacMillan, *J. Org. Chem.* **2016**, *81*, 6898–6926.

[9] B. Zhang, A. Studer, *Chem. Soc. Rev.* **2015**, *44*, 3505–3521.

[10] C. Russo, F. Brunelli, G. Cesare Tron, M. Giustiniano, *Chem. Eur. J.* **2023**, *29*, e202203150.

[11] C. Russo, J. Amato, G. C. Tron, M. Giustiniano, *J. Org. Chem.* **2021**, *86*, 18117–18127.

[12] C. Russo, G. Graziani, R. Cannalire, G. C. Tron, M. Giustiniano, *Green Chem.* **2022**, *24*, 3993–4003.

[13] N. L. Reed, T. P. Yoon, *Chem. Soc. Rev.* **2021**, *50*, 2954–2967.

[14] Albeit a common PET pathway is more likely, it is not possible to a priori exclude an energy transfer event.

[15] W. Liang, S. A. Fischer, M. J. Frisch, X. Li, *J. Chem. Theory Comput.* **2011**, *7*, 3540–3547.

[16] R. E. Stratmann, G. E. Scuseria, M. J. Frisch, *Citation: J. Chem. Phys* **1998**, *109*, 8218.

[17] A. Dreuw, M. Head-Gordon, *Chem. Rev.* **2005**, *105*, 4009–4037.

[18] M. E. Casida, Time-Dependent Density Functional Response Theory for Molecules. In Recent Advances in Density Functional Methods: (Part I), Vol. 1; Chong, D. P., Ed.; World Scientific Publishing: Singapore, **1995**; pp 155−193.

[19] J. Choi, H. Kim, *J. Chem. Theory Comput.* **2021**, *17*, 767–776.

[20] T. B. Demissie, K. Ruud, J. H. Hansen, *Organometallics* **2015**, *34*, 4218–4228.

[21] D. D. Méndez-Hernández, P. Tarakeshwar, D. Gust, T. A. Moore, A. L. Moore, V. Mujica, *J. Mol. Model.* **2013**, *19*, 2845–2848.

[22] A. Kuhn, K. G. Von Eschwege, J. Conradie, *J. Phys. Org. Chem.* **2012**, *25*, 58–68.

[23] S. S. Yamijala, G. Periyasamy, S. K. Pati, *J. Phys. Chem.* **2011**, *115*, 12298–12306.

[24] M. Pastore, S. Fantacci, F. De Angelis, *J. Phys. Chem.* **2010**, *114*, 22742–22750.

[25] M. K. Nazeeruddin, F. De Angelis, S. Fantacci, A. Selloni, G. Viscardi, P. Liska, S. Ito, B. Takeru, M. Grätzel, *J. Am. Chem. Soc.* **2005**, *127*, 16835–16847.

[26] A. Maccoll, *Nature* **1949**, *163*, 178–179.

[27] J. A. Milligan, J. P. Phelan, S. O. Badir, G. A. Molander, *Angew. Chem. Int.Ed.* **2019**, *58*, 6152–6163.

[28] B. Bieszczad, L. A. Perego, P. Melchiorre, *Angew. Chem. Int. Ed.* **2019**, *58*, 16878–16883.

[29] E. Gandolfo, X. Tang, S. Raha Roy, P. Melchiorre, *Angew. Chem. Int. Ed.* **2019**, *58*, 16854–16858.

[30] G. Suresh Yedase, S. Venugopal, P. Arya, V. Reddy Yatham, *Asian J. Org. Chem.* **2022**, *11*, e202200478.

[31] P. Z. Wang, J. R. Chen, W. J. Xiao, *Org. Biomol. Chem.* **2019**, *17*, 6936–6951.

[32] W. Huang, X. Cheng, W. Huang Xu Cheng, O. R. Br, *Synlett* **2017**, *28*, 148–158.

[33] W. Schilling, D. Riemer, Y. Zhang, N. Hatami, S. Das, *ACS Catal.* **2018**, *8*, 5425–5430.

[34] Y. M. Poronik, B. Sadowski, K. Szychta, F. H. Quina, V. I. Vullev, D. T. Gryko, *J. Mater. Chem. C Mater.* **2022**, *10*, 2870–2904.

[35] M. C. Chen, D. G. Chen, P. T. Chou, *Chempluschem* **2021**, *86*, 11–27.

[36] J. C. Tellis, D. N. Primer, G. A. Molander, *Science* **2014**, *345*, 433–436.

[37] J. K. Matsui, S. B. Lang, D. R. Heitz, G. A. Molander, *ACS Catal.* **2017**, *7*, 2563–2575.

[38] G. A. Molander, D. L. Sandrock, *Curr. Opin. Drug Discov. Devel.* **2009**, *12*, 811.

[39] T. Caronna, G. Fronza, F. Minisci, O. Porta, *J. Chem. Soc., Perkin Trans. 2* **1972**, 2035–2038.

[40] J. Liu, Q. Liu, H. Yi, C. Qin, R. Bai, X. Qi, Y. Lan, A. Lei, *Angew. Chem. Int. Ed.* **2014**, *53*, 502–506.

[41] G. N. Papadopoulos, D. Limnios, C. G. Kokotos, *Chem. Eur. J.* **2014**, *20*, 13811–13814.

[42] L. Chu, J. M. Lipshultz, D. W. C. Macmillan, *Angew. Chem. Int. Ed.* **2015**, *54*, 7929–7933.

[43] H. Tan, H. Li, W. Ji, L. Wang, *Angew. Chem. Int. Ed.* **2015**, *54*, 8374–8377.

[44] For an exhaustive review about acyl-transfer reactions involving α-keto acids see: F. Penteado, E. F. Lopes, D. Alves, G. Perin, R. G. Jacob, E. J. Lenardão, *Chem. Rev.* **2019**, *119*, 7113–7278.

[45] R. Cannalire, S. Pelliccia, L. Sancineto, E. Novellino, G. C. Tron, M. Giustiniano, *Chem. Soc. Rev.* **2021**, *50*, 766-897.

[46] C. H. Hu, Y. Li, *J. Org. Chem.* **2023**, *88*, 6401-6406.

[47] T. Pirali, M. Serafini, S. Cargnin, A. A. Genazzani, *J. Med. Chem.* **2019**, *62*, 5276–5297.

[48] A. Dewanji, C. Mück-Lichtenfeld, K. Bergander, C. G. Daniliuc, A. Studer, *Chem. Eur. J.* **2015**, *21*, 12295–12298.

[49] A. H. Lipshutz, T. B. Petersen, A. R. Abela, *Org. Lett.* **2008**, *10*, 1333–1336.

[50] P. Patil, M. Ahmadian-Moghaddam, A. Dömling, *Green Chem.* **2020**, *22*, 6902–6911.

[51] J. G. Polisar, J. R. Norton, *Tetrahedron* **2012**, *68*, 10236–10240.

[52] A. Mayr, L. F. Mao, *Inorg. Chem.* **1998**, *37*, 5776–5780.

[53] X. Wang, Q. G. Wang, Q. L. Luo, *Synthesis* **2015**, *47*, 49–54.

[54] S. Zhou, K. Lv, R. Fu, C. Zhu, X. Bao, *ACS Catal.* **2021**, *11*, 5026–5034.

[55] W. Liu, P. Liu, L. Lv, C. J. Li, *Angew. Chem. Int. Ed.* **2018**, *57*, 13499–13503.

[56] W. W. Zhao, Y. C. Shao, A. N. Wang, J. L. Huang, C. Y. He, B. D. Cui, N. W. Wan, Y. Z. Chen, W. Y. Han, *Org. Lett.* **2021**, *23*, 9256–9261.
[57] S. Xie, D. Li, H. Huang, F. Zhang, Y. Chen, *J. Am. Chem. Soc.* **2019**, *141*, 16237–16242.
[58] P. G. Li, H. Zhu, M. Fan, C. Yan, K. Shi, X. W. Chi, L. H. Zou, *Org. Biomol. Chem.* **2019**, *17*, 5902–5907.
[59] K. Wadhwa, C. Yang, P. R. West, K. C. Deming, S. R. Chemburkar, R. E. Reddy, *Synth. Commun.* **2008**, *38*, 4434–4444.
[60] V. V. Voronin, M. S. Ledovskaya, K. S. Rodygin, V. P. Ananikov, *Org. Chem. Front.* **2020**, *7*, 1334–1342.
[61] G. Zhao, Y. Wang, C. Wang, H. Lei, B. Yi, R. Tong, *Green Chem.* **2022**, *24*, 4041–4049.
[62] F. Tobita, T. Yasukawa, Y. Yamashita, S. Kobayashi, *Catal. Sci. Technol.* **2022**, *12*, 1043–1048.
[63] H. Li, C. D. Sibley, Y. Kharel, T. Huang, A. M. Brown, L. G. Wonilowicz, D. R. Bevan, K. R. Lynch, W. L. Santos, *Bioorg. Med. Chem.* **2021**, *30*, 115941.
[64] L. Liu, Y. Liu, X. Shen, X. Zhang, S. Deng, Y. Chen, *J. Org. Chem.* **2022**, *87*, 6321–6329.
[65] R. S. Ghogare, *Org. Commun.* **2020**, *13*, 103–113.
[66] J. Dong, X. Wang, Z. Wang, H. Song, Y. Liu, Q. Wang, *Chem. Sci.* **2020**, *11*, 1026–1031.
[67] A. D. Becke, *J. Chem. Phys.* **1998**, *98*, 5648.
[68] A. Lee, W. Yang, R. G. Parr, *Phys. Rev. B* **1988**, *37*, 785.
[69] M. Gussoni, M. N. Ramos, C. Castiglioni, G. Zerbi, *Chem. Phys. Lett.* **1989**, *160*, 200–205.
[70] Gaussian 16, Revision A.03, M. J. Frisch, G. W. Trucks, H. B. Schlegel, G. E. Scuseria, M. A. Robb, et al., Gaussian, Inc., Wallingford CT, 2016.
[71] B. Miehlich, A. Savin, H. Stoll, H. Preuss, *Chem. Phys. Lett.* **1989**, *157*, 200−206.
[72] W. Fan, D. Tan, W.-Q. Deng, *ChemPhysChem* **2012**, *13*, 2051-2060.
[73] G. Donati, A. Petrone, P. Caruso, N. Rega, *Chem. Sci.* **2018**, *9*, 1126-1135.
[74] A. Petrone, P. Cimino, G. Donati, Hrant P. Hratchian, M. J. Frisch, N. Rega, *J. Chem. Theory Comput.* **2016**, *12*, 4925–4933.
[75] S. Miertuš, E. Scrocco and J. Tomasi, *Chem. Phys.* **1981**, *55*, 117–129.
[76] B. Mennucci and J. Tomasi, *J. Chem. Phys.* **1997**, *106*, 5151– 5158.
[77] N. Rega, M. Cossi and V. Barone, *Chem. Phys. Lett.* **1998**, *293*, 221–229.
[78] GaussView, Version 6.1, Roy Dennington, Todd A. Keith, and John M. Millam, Semichem Inc., Shawnee Mission, KS, 2016.
[79] P.J. Turner, XMGRACE, Version 5.1.19. Center for Coastal and Land-Margin Research, Oregon Graduate Institute of Science and Technology, Beaverton, OR; 2005.

10.1002/chem.202301852

WILEY VCH

RESEARCH ARTICLE

Entry for the Table of Contents

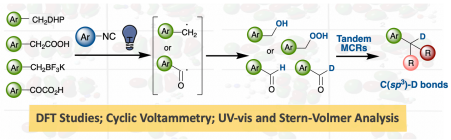

Aromatic isocyanides are able to harvest visible light and promote the oxidative formation of both alkyl and acyl radicals starting from Hantzsch esters, potassium alkyltrifluoroborates, and α-oxoacids. UV-visible absorption and fluorescence experiments, electrochemical measurements along with computational calculations provided key data for mechanistic insights. Furthermore, a direct and easy access to deuterium labeled compounds have also been reported.

Institute and/or researcher Twitter usernames: @giustiniano